T.R.
GEBZE TECHNICAL UNIVERSITY
ENERGY TECHNOLOGIES INSTITUTE

EXPERIMENTAL INVESTIGATION OF THERMOPHYSICAL PROPERTIES OF CERAMIC MOLDS IN INVESTMENT CASTING

AYÇA ŞEYMA BİRDAL
A THESIS SUBMITTED FOR THE DEGREE OF
MASTER OF SCIENCE
APPLIED PROPULSION SYSTEM DESIGN & ENGINEERING
FOR AEROSPACE TECHNOLOGIES DEPARTMENT

GEBZE
2022

T.R.

GEBZE TECHNICAL UNIVERSITY

ENERGY TECHNOLOGIES INSTITUTE

EXPERIMENTAL INVESTIGATION OF THERMOPHYSICAL PROPERTIES OF CERAMIC MOLDS IN INVESTMENT CASTING

AYÇA ŞEYMA BİRDAL

A THESIS SUBMITTED FOR THE DEGREE OF MASTER OF SCIENCE

APPLIED PROPULSION SYSTEM DESIGN & ENGINEERING FOR AEROSPACE TECHNOLOGIES DEPARTMENT

THESIS SUPERVISOR

Asst. Prof. MAHMUT AKŞİT

GEBZE

2022

GEBZE TEKNİK ÜNİVERSİTESİ	**YÜKSEK LİSANS JÜRİ ONAY FORMU**

GTÜ Energy Teknolojileri Enstitüsü Yönetim Kurulu'nun 27/06/2022 tarih ve 2022/09 sayılı kararıyla oluşturulan jüri tarafından 26/07/2022 tarihinde tez savunma sınavı yapılan Ayça Şeyma BİRDAL'ın tez çalışması Enerji Teknolojileri Anabilim Dalında YÜKSEK LİSANS tezi olarak kabul edilmiştir.

JÜRİ

ÜYE
(TEZ DANIŞMANI) : Dr. Mahmut AKŞİT

ÜYE : Prof. Dr. İlyas KANDEMİR

ÜYE : Dr. Mehmet Ekrem ÇAKMAK

ONAY

Gebze Teknik Üniversitesi Fen Bilimleri Enstitüsü Yönetim Kurulu'nun

...../...../…… tarih ve ……/…..... sayılı kararı.

SUMMARY

Investment casting enables the casting of complex metal parts at high dimensional accuracy with near net shape and high surface quality, as typically required by the aerospace industry. The most critical process in investment casting is shelling. In this process, the wax assembly is dipped into the ceramic slurry and powdered with refractory materials consecutively for each ceramic shell layer until the desired number of layers and/or total shell thickness is obtained. Because there are gas and heat transfers between the ceramic mold, molten alloy, and surrounding environment during casting, the thermophysical properties of the ceramic mold significantly affect the metal solidification morphology and the application performance of the end-product. Prediction of the investment casting results with casting simulation before the actual casting is very important for reducing project time and cost. However, casting simulations are rarely used in the investment casting industry because of challenges associated with providing necessary reliable parametric input to simulation software. The motivation of this study is to measure and analyze the thermophysical properties of the ceramic mold in investment casting by experimental methods.

Ceramic shell coatings utilized in the aluminum production line of a Turkish investment casting foundry are investigated in this work. The thermophysical properties such as specific heat, density, and gas permeability are measured and analyzed for these ceramic molds. Three different ceramic shell molds are prepared, measured, and analyzed: A) Ceramic mold that only consists of prime coating, B) Ceramic mold that only consists of backup coating, and C) Ceramic mold that consists of both the prime and backup coating. The densities are measured with He-pycnometer. The specific heats are measured with Differential Scanning Calorimetry (DSC). The gas permeability measurements are performed with the in-house built set-up.

Key Words: Investment Casting, Ceramic Mold, Thermophysical Properties, Specific Heat, Density, Gas Permeability

ÖZET

Hassas döküm tipik olarak havacılık endüstrisinin gerektirdiği şekilde, karmaşık metal parçaların yüksek boyutsal doğrulukta, net şekle yakın ve iyi yüzey kalitesiyle dökümünü sağlar. Hassas döküm metodunda en kritik süreç seramik kalıp oluşturmadır. Bu işlemde, mum salkımı istenen kat sayısına ve/veya seramik kalınlığına ulaşılıncaya kadar art arda seramik bulamaca daldırılır ve refrakter kum ile kaplanır. Döküm sırasında seramik kalıp, ergimiş metal ve ortam arasında gaz ve ısı transferleri olduğundan seramik kalıbın termofiziksel özellikleri metal katılaşma morfolojisini dolayısıyla da nihai ürünün uygulama performansını önemli ölçüde etkiler. Döküm öncesi simülasyon ile hassas döküm sonuçlarının tahmin edilmesi, projenin geliştirme faaliyetleriyle birlikte terminini ve maliyetini azaltmak için çok önemlidir ancak simülasyon yazılımına gerekli güvenilir parametrik girdiyi sağlamayla ilgili zorluklar nedeniyle döküm simülasyonları, hassas döküm endüstrisinde nadiren kullanılmaktadır. Bu çalışmanın amacı, hassas döküm seramik kalıbının termofiziksel özelliklerinin deneysel yöntemlerle analiz edilmesidir.

Bu çalışmada bir Türk Hassas Döküm Firmasının alüminyum üretim hatlarında kullanılan seramik kalıpları incelenmiştir. Bu seramik kalıplar için özgül ısı, yoğunluk ve gaz geçirgenliği gibi termofiziksel özellikler ölçülerek analiz edilmiştir. Üç farklı seramik kalıp hazırlanmış, ölçümleri yapılmış ve analiz edilmiştir. Bunlar: A) Sadece ilk kat banyosu kullanılarak hazırlanan seramik kalıp, B) Sadece arka kat banyosu kullanılarak hazırlanan seramik kalıp, C) Hem ilk kat hem de arka kat banyosunu içeren ve standart uygulama prosedürüne göre hazırlanan seramik kalıp. Yoğunluklar He-piknometresi ile, özgül ısı değerleri Diferansiyel Taramalı Kalorimetre (DSC) ile ve gaz geçirgenlikleri laboratuvar ortamında hazırlanan düzenek ile elde edilmiştir.

Anahtar Kelimeler: Hassas Döküm, Seramik Klıp, Termofiziksel Özellikler, Özgül Isı, Termal İletkenlik, Yoğunluk, Gaz Geçirgenliği

ACKNOWLEDGEMENTS

First of all, I want to express my special thanks to my advisor, Dr. Mahmut AKSIT, who has always supported me in my thesis by sharing his knowledge and experience with me. I would also like to thank my co-advisor Cansinem TUZEMEN GUNDOGAN for her encouragement in my studies.

I would like to extend my thanks to Mr. Gursel YARDIMCI who is General Manager of Gurmetal Investment Casting Company for enabling such a master of science opportunity to start while I was working in his company. I would also like to thank each of my colleagues who supported me throughout my studies.

I owe a warm thanks to laboratory personnel in Characterization Analysis Laboratory-1 of Aluminum Research and Application Center and Mechanical Testing Laboratory of Materials Science and Engineering Department at GTU for their valuable support in conducting my experimental studies. I owe a very special thanks to M.Sc. and Ph.D. students in Materials Physics Laboratory for their help and friendship.

I would especially like to thank my dear parents and dear brother who trusted me and gave me strength with their presence, and my friends who were always there for me throughout my master's degree.

Finally, special thanks to Onur BALAK for his presence, understanding, endless support, and unconditional love.

TABLE OF CONTENTS

LIST OF ABBREVIATIONS AND ACRONYMS

Abbreviations and Acronyms		**Explanations**
α	:	Thermal Diffusivity
Avg.	:	Average
B.C.	:	Before Christ
CAD	:	Computer-aided Design
CFD	:	Computational Fluid Dynamics
cp	:	Specific Heat
DSC	:	Differential Scanning Calorimetry
e.g.	:	For example
$etc.$	:	And the rest
$i.e.$	:	That is
GTU	:	Gebze Technical University
HIP	:	Hot Isostatic Pressing
K_0	:	Thermal Conductivity of Dense Ceramic Body
K	:	Thermal Conductivity of Porous Ceramic Body
k	:	Thermal Conductivity
LFA	:	Laser Flash Method
Min.	:	Minute
mm	:	Milimeter
n	:	A Constant Depending on Pore Structure and Topology
NDT	:	Non Destructive Testing
ρ	:	Bulk Density
P	:	Volume Fraction of Pores
SEM	:	Scanning Electron Microscopy
Temp.	:	Temperature
UK	:	United Kingdom
ZKE	:	Hydrolyzed Ethyl Silicate
φ	:	Porosity

LIST OF FIGURES

LIST OF TABLES

1. INTRODUCTION

Metal casting enables manufacturing of requested shaped parts by pouring or forcing molten metal into molds without performing extra forming operations such as rolling or forging. It has a long historical background because of being one of the oldest industries both in ancient and medieval history periods. However, except the studies of a few scientists, metal casting was accepted as an art and this judgement was remained by the twentieth century [1].

Proper metal casting method to manufacture requested shaped parts are determined based on the casting characteristics such as casting weight interval, geometric complexity of part, requested alloy composition, metal tooling cost etc. Investment casting process also known as cire-perdue, lost-wax or precision casting is one of the oldest metal casting processes that shows itself back in 5000 B.C. with rudimentary items. However, urgent demand for war equipment during the World War II in the United States revealed the importance of the investment casting as the capacity of the machine tool industry could not meet high-need finished products for defense and aircraft parts. In particular, aircraft gas turbine applications have accelerated the production and development of investment castings due to the need for turbine blades that withstand high temperatures and hence require refractory alloys [2].

Investment casting mainly initials with metal tool design and tool manufacturing steps. When the metal tool is manufactured and validated, the decomposable molten wax is injected into the tool at 60-70ºC and at 500-1000 psi pressure [3] to form wax patterns that reflect exact part geometry. After injection of waxes and waiting for their solidification, the wax models are assembled with other wax components such as pouring cups, gating, and runner to form a casting tree.

The second main step of investment casting is to create a decomposable ceramic shell mold to form a casting cavity. For this construction, ceramic slurry which involves fine mesh refractory materials and binders is “invested” around the casting tree and this casting tree is powdered with coarse mesh refractory materials after dipping into slurry [4]. Hence, ceramic shell molding consists of two sub-processes.

The first one is the dipping/investing process and the second one is the coating/stuccoing process. Each time, first, the entire wax tree is dipped into a ceramic slurry tank to produce a uniform ceramic mold. Second, the wax tree is coated with the powder of the investment/molding mixture. The ceramic mold is then allowed to dry between each layer. The dipping and stuccoing processes are repeated until a ceramic mold thickness reaches ~ 6-8 mm [3].

Once the ceramic mold has dried enough in a controlled atmosphere, the wax inside of the mold shall be removed to reveal the ceramic shell cavity for casting. This step is called dewaxing and is accomplished by heating the mold to a reasonable temperature that allows the wax to melt. The mold is placed in the autoclave upside down to allow the wax removal. In general, the mold is placed at a temperature of 180ºC - 200ºC for about 15 min. in an autoclave of molten wax [5]. The ceramic mold is then burned out at 870°C - 1095°C to remove any moisture and residual wax, and to sinter the mold [6].

One other process before casting is preheating. The preheating process provides homogenized temperature to the mold. This allows molten metal to stay liquid longer and to fill every detail because of the mold and casting cool together [6]. In the casting step, both air and vacuum casting methods can be used. Air casting is preferred for aluminum, magnesium, copper, gold, silver, platinum, all types of steel, ductile iron, most cobalt alloys, and nickel-base alloys that do not contain reactive elements. On the other hand, vacuum casting is preferred for γ'-strengthened nickel base alloys, some cobalt alloy, titanium, and refractory metals since this casting provides cleaner metals with superior properties and is used for alloys that cannot be cast in the air [7].

After casting and solidification, post-casting operations are conducted. These are knock out to remove ceramic mold from casting, cut off the metal mold to separate gating and casting part if needed core removal to distract core from casting, heat treatment to provide mechanical requirements and stress relief, abrasive cleaning to leave casting as clean condition, etc. Some other post-casting operations are hot isostatic pressing (HIP) is being increasingly adopted to eliminate porosity, and to

improve properties, especially for titanium, and used optionally for steel, aluminum, and superalloys [7].

Main steps of the investment casting are given in Figure 1.1.

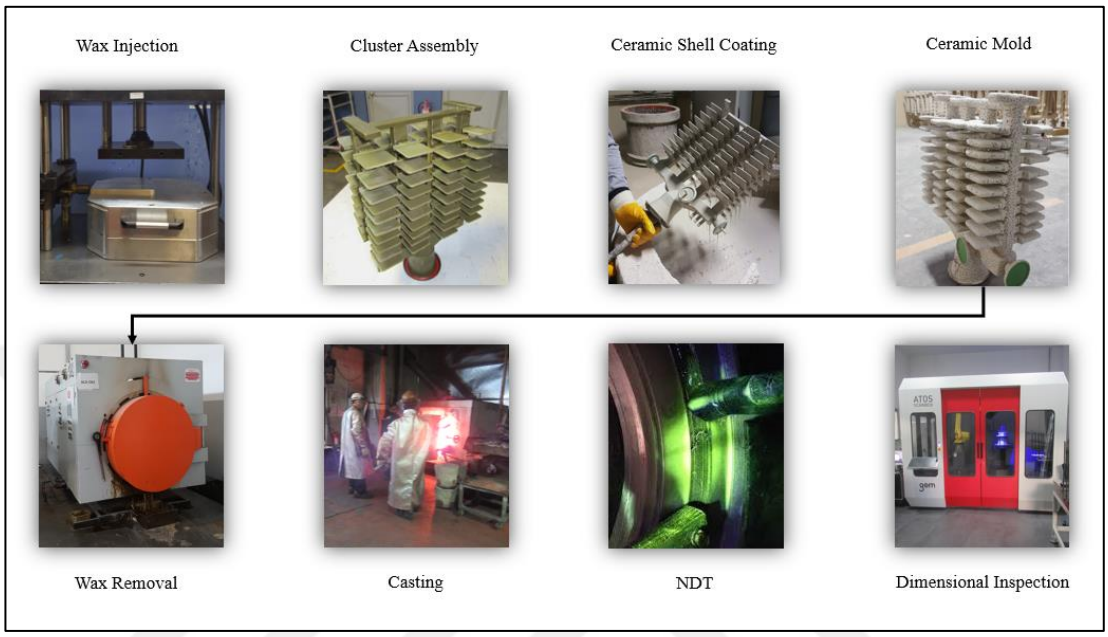

Figure 1. 1 Main steps of the investment casting.

1.1. Motivation of Research

The most critical process in investment casting is ceramic shell molding because the dimensions and quality of castings depend on this structure. This process is often company specific. All the know-how and experience are confidential in the company. In addition, it is an expensive process and involves many parameters that need to be aware of and in control of. Otherwise, the properties of ceramic molds change day by day, and the products may be in suspicious condition because of the lack of process control.

1.2. Objective and Impact of Research

Many attempts are made to achieve good casting results. However, to perform and wait to see trial results are quite inefficient in terms of cost and time. At this step, the use of computer solidification simulation software reveals its importance. There

are many alternative computer simulation software systems that use heat and gas transfer models with finite element or finite volume methods. These are being utilized in the design of cluster assembly of waxes, gating, and feeding systems to show the filling and solidification journey of molten metal through the mold during filling and solidification and this provides a prediction of casting results before actual casting [7].

The objective of this thesis is to investigate the thermophysical properties of ceramic molds of investment casting with experimental methods in order to improve product development processes.

1.3. Outline of Thesis

This thesis is divided into six chapters. Chapter 1 describes the historical process of investment casting and the steps of this casting method. This chapter also explains the motivation, objective, and impact of this research. Chapter 2 presents the previous research and the approaches to similar issues. Chapter 3 describes the methodology used in the design of the experiments. Chapter 4 focuses on the results of each experimental study. Chapter 5 discusses the results. Finally, Chapter 6 summarizes the main conclusions of this thesis and presents an outlook for the possible extensions of the research in the future.

2. LITERATURE REVIEW

2.1. Ceramic Molds General Considerations

All molds are constructed from three components. These are the binder, filler, and stucco materials. Binders include two groups water-based and alcohol-based. On the other hand, many ceramics are used for the filler and stucco. There are various combinations for the slurry and the stucco and there is no hard rules exist as to the correct combination. This choice depends on the alloy to be cast, the casting quality, and the dimensional accuracy desired. In addition to these, economical and environmental aspects are also considered [8]

Before starting the ceramic shell molding process, multi-component slurries are prepared that involves a filler system with a fine mesh refractory and a colloidal binder system. Once the slurries are ready for the process, the casting tree is dipped into the slurry that consists of a suspension of refractory powders in liquid binder solutions. After each layer, except for the seal coat, the casting tree is powdered with granular refractory material to form stucco layers and dried in a humidity and temperature-controlled atmosphere [9].

Generally, the ingredients as the type of ceramic filler and the binder liquid of primary and backup coats are different from each other since the duties of primary coat differ from backup coats. The primary coat is to be in contact with molten metal. On the other hand, backup coats form the shell thickness, and both the effects of their combination and the bulk properties of the ceramic mold. Since the slurry composition of the primary coat needs to be impermeable, refractory and chemically inert zirconium silicate or zircon is used mostly for prime coat filler. Colloidal silica is one of the preferred binders as it provides stable yields in strong particle-particle binding in fillers. Filler examples can be mullite, zircon, and cobalt aluminates [8].

The stuccoing is another important application during ceramic shell molding. The reason behind of utilization of stucco is to reduce drying stresses in the shell forming many stress concentration centers that distribute and hence decrease the

magnitude of local drying stress in the mold. In addition to this duty of stucco, it also provides a rough surface between the primary and backup coats, thus bonding of each layer gets easy. Once the primary coat is air-dried, the casting tree is consecutively dipped into a backup slurry and stuccoed until the required thickness or layer of the ceramic mold is achieved [10], [11]. The majority of casting foundries use zircon stucco for a primary coat. There are many benefits of using fined-grained zircon such as high surface quality, good flowability, and drain ability because of its round shape and heavy density, low thermal expansion coefficient for dimensional stability, low reactiveness with molten metals, etc [12].

Despite the majority of larger companies using water-based colloidal silica binders, a less quantity of UK foundries are using alcohol-based binders because of environmental hazards even though mixing and drying times are faster than water-based binders. On the other hand, water-based binders need much longer drying and mixing time but they are more popular due to their dimensional stability, chemical inertness, and environment friendliness properties [13]. At the end of ceramic shell molding, a seal coat is given to hold the last stucco. Figure 2.1 shows a schematic of a ceramic shell mold for investment casting.

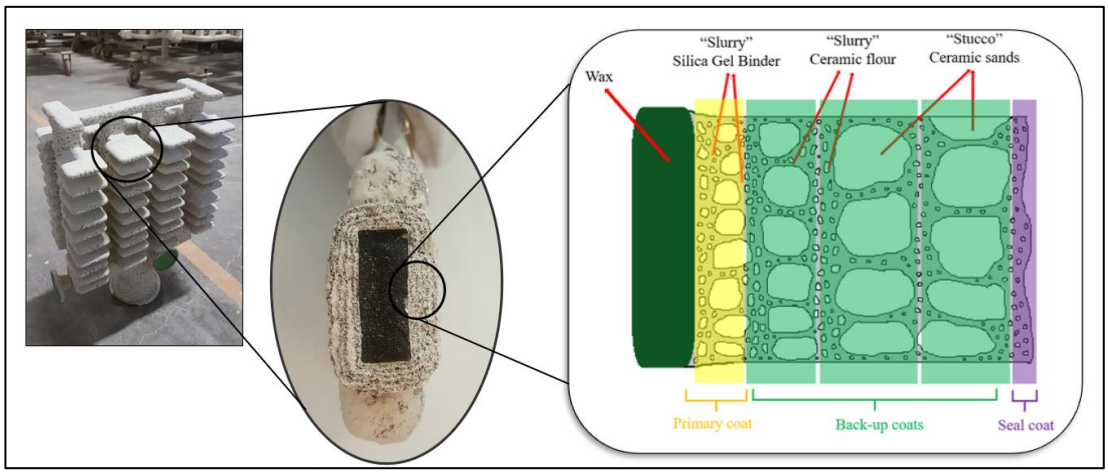

Figure 2. 1 Schematic of a ceramic shell mold for investment casting.

There are substantial expectations from an investment casting ceramic mold. The first is sufficient green strength. It is important for withstanding wax removal without failure such as major cracks or breaking of some part of the ceramic mold. The second is sufficient fired strength because the mold carries the weight of cast metal.

The third is high thermal shock resistance since thermal shock resistance prevents hot-tearing while casting. The fourth is high chemical stability. Ceramic mold materials could have a tendency for chemical interaction. However, chosen chemical inertness combinations of slurries and stuccos considering alloy type prevent this interaction between molten alloy and ceramic mold. Thermal conductivity and permeability are also essential properties of ceramic molds. There is thermal transfer through the ceramic mold and this allows metal cooling. Mold permeability and thermal conductivity shall be sufficient for this thermal transfer. Solidification also determines the dimensional features of the casting products. For this reason, thermal expansion is an essential mold property that is to be considered to limit dimensional changes of the casting product [10].

2.2. Thermophysical Properties of Ceramic Molds

Thermophysical properties of investment casting ceramic shell molds have a significant influence on the solidification of molten metal and hence affect the properties of the casting product. The term thermophysical signifies the physical properties of materials that are affected by elevated temperatures such as specific heat, thermal diffusivity, thermal conductivity and density. Specific heat and density are in the subject of this thesis. In addition to these, gas permeability feature was included to this study.

There is a theoretical approach between the most important thermophysical properties of a material which are thermal conductivity, thermal diffusivity, specific heat and density.

The approach between these properties is given by:

$$\alpha = \frac{\mathbf{k}}{\boldsymbol{\rho cp}} \qquad \textbf{Equation 2. 1}$$

where:

α = thermal diffusivity ($\frac{m^2}{s}$),

k = thermal conductivity ($\frac{W}{m\ K}$),

ρ = bulk density ($\frac{kg}{m^3}$),

cp = specific heat ($\frac{J}{kg\ K}$) [14].

On the other hand, there are many equations related to the interaction between porosity and thermal conductivity which are submitted by some researchers. The amount of porosity expresses the gas permeability property of the material. In 1975 researcher S.K Rhee concluded that Aivazov and Domashnev equation better describes the effect of porosity on thermal conductivity.

Aivazov and Domashnev's equation is given by:

$$\frac{K}{K_0} = \frac{1-P}{1+nP^2}$$ **Equation 2. 2**

where:

K = thermal conductivity of porous ceramic body,

K_0 = thermal conductivity of dense ceramic body,

P = volume fraction of pores,

n = a constant depending on pore structure and topology.

Domashnev equation indicates the correlation between porosity and thermal conductivity [15].

2.2.1. Specific Heat

Specific heat is one of the thermophysical properties of ceramic shell molds in high temperature applications and casting solidification is affected by this thermophysical property of the ceramic mold. While a molten metal is flowing in a ceramic mold, the temperature changes, and this temperature difference affects the quality of casting. When molten metal solidifies, the liquid phase transforms into the solid phase at the solidification temperature. During that solidification, a kind of energy is being released into the environment and this energy is called latent heat. The area that is exposed to released latent heat is affected by this energy [16]. Hence, the underlying cause of specific heat effects on solidification is directed to superheat and latent heat concepts. Castings with 5-15 mm wall thicknesses accumulate most of superheat and part of the latent heat of molten metal in ceramic shell mold. At this stage, specific heat plays an important role. This factor is significant to control shrinkage and some other casting defects [17].

It is very simple to determine this thermodynamic quantity for small and homogeneous samples. However, the determination of this property for heterogeneous samples with large pores is highly constrained [18].

2.2.2. Density

Density is another thermophysical property of ceramic shell molds that has crucial importance in casting solidification. Because the density of the ceramic shell mold is supposed to change only slightly over interesting temperatures its temperature dependence was not accounted for [19].

Saridikmen et al. 2005 [20] studied the structural and physical properties of ceramic casting molds produced with two different binder compositions. These compositions included ethyl silicate [$C_8H_{20}O_4Si$] and ethyl silicate with aluminum tri-sec-butoxide [$Al(OCH(CH_3) - C_2H_5)_3$]. For stuccoing process zircon was used. After sintering, the authors [20] determined the porosity, sintering shrinkage, density and hardness of the molds. In addition, surface morphology was investigated by Scanning Electron Microscopy (SEM) and phase structures were examined by EDAX spectrometer. As a result of the analysis, it was found that increasing sintering temperature and time decreases the porosity and increases the shrinkage of the mold and hence increases the bulk density for two binders. It was also seen that despite having very similar porous microstructure, the molds give different surface qualities to the casting products. However, the authors [20] found that [$Al(OCH(CH_3) - C_2H_5)_3$] binder system produces ceramic molds with homogeneously distributed pores. These pores ensure the gas removal during casting. The authors [20] observed better surface quality from the molds which have low porosity and high bulk density and were constructed with [$Al(OCH(CH_3) - C_2H_5)_3$] binders.

2.2.3. Gas Permeability

Gas permeability is a physical property of ceramic shell molds that has strong importance in casting qualification.

There are many kinds of ceramic shell compositions. Due to this variety of shell compositions, generally ceramic molds have 10-30 % porosity. The porosity provides air permeability to ceramic mold. On the other hand, it also affects the mechanical and thermal properties of the ceramic mold.

There is an approach to estimating the effect of porosity on the thermal conductivity of ceramic molds.

This approach is given by:

$$\mathbf{k_r} = \exp \frac{(-1.5\,\varphi)}{(1-\varphi)} \qquad \textbf{Equation 2. 3}$$

Where;

φ = porosity,

$k_r = \frac{k}{k_0}$ relative thermal conductivity, with k denoting the effective thermal conductivity of the porous material,

k_0 = denoting the thermal conductivity of the dense solid material [21]**.**

Kline et al. 2010 [22] studied to increase the permeability of an investment casting mold using decomposable pore formers. They [22] focused on the simulation of thin-layer ceramic shell molding with relatively large-scale pores beside their experimental results in the laboratory. The experimental results were highly important since the simulation works based on the monolithic structure and random particle dispersion however ceramic shell molding has multiple layers and stucco between each layer except for the seal coat. To build a correlation between the experimental results and the simulation results, multiple layer test samples were prepared and analyzed. They [22] used a refractory slurry that involves fused silica flour and colloidal silica binder and also graphite particles. At the end of the shelling process, the ceramic shell mold was fired to remove the graphite particles, and pores were revealed in situ of graphite particles. The authors [22] used the digital permmeter to measure the gas permeability of the ceramic shell mold. The authors [22] used the three-dimensional Monte Carlo and CFD simulations and they used the experimental mold properties taken from samples created for this study. The pore quantities predicted with Monte Carlo simulations were multiplied by the airflow rate with CFD models to obtain an average airflow rate through the cuboid. As a result of these analyses, permeability-pore density-layer height correlation curves were obtained. The authors [22] compared

the simulation results and the experimental results. They observed that the simulation results are a good representation of the experimental results and the results show that the permeability of ceramic molds increases exponentially when there are more concentrated pores.

Wisniewski et al. 2020 [23] determined the properties of quartz powders, nano silica dioxide binders, and multilayer samples of ceramic molds. They [23] used two types of multilayered ceramic molds that consist of seven layers and the ceramic molds were created with silica powder-based refractory slurry. As polymer binder, they [23] used ZKE, LUDOX PX30, Remasol Plus, and Remasol Premium (Remet, UK) containing colloidal SiO_2. This study includes two different particle sizes of silica sand for stucco. 0.1-0.3 mm for the first two layers, and 0.5-1.0 mm for the structural layers. An in-house built gas permeability test device was used. In this study, the authors [23] compared two types of seven-layer ceramic molds. The first type was created with the combination of an alcohol system based on ZKE (layers 1, 2, 5, 7) and LUDOX PX 30 water binder (layers 3, 4, 6). The second type was created with a water-based system only with Remasol binders. The authors [23] observed that the second type has a higher porosity in the raw state and the amount of porosity increased after firing. Furthermore, it is almost twice as high as the first type in the fired state. However, despite this difference between the porosity results, the gas permeability results of the two types of molds are almost the same. The authors [23] concluded that the second type of mold has more advantageous and promising properties than the first type of mold.

2.3. Product Development Processes in Investment Casting

Casting product development processes initial with the design step. Designing for manufacture comes first. This step starts from a concept idea or an outline drawing and design teams provide detailed drawings to finalize design requirements. CAD technology via Solidworks displays the final product. The second step is simulation. Once the product designs have been completed, a full casting simulation is run to achieve reliable casting simulation ensuring that the quality of casting is maintained. CAD models are used to simulate filling and solidification. This minimizes actual casting trials and decreases the vanity due to actual casting trials. In that way, using simulation software and achieving reliable results decrease the cost of development processes. The last step is development. Once the product is designed and the simulation is run for casting, engineering teams discussed the progress to the development step. This discussion is about material options, dimensional tolerance considerations, cost-saving discussions, etc. [24]. An actual casting trial takes a minimum of 3 weeks to achieve as-cast results. This duration may be longer and there may be some consequences that require tooling modifications and this reveals additional costs.

Considering the time and cost of actual casting trials, it is obvious that the simulation step of investment casting product development processes is quite a lot important. Determining parameters that need to be measured and fed into the software shall be useful for the integration of software into the company's casting atmosphere. This work requires long-termed, patient, and precise effort for the integration to obtain reasonable, logical, and reliable results. Using that software is inevitable. Otherwise, getting through such limited product requirements takes a long time and brings additional costs [25].

2.4. Simulation of Investment Casting General Considerations

Using simulation software is an enormously productive method to shorten the new product development cycle and minimize the production cost when compared with an actual casting trial and error. While using simulation programs, the analysis of the casting process is not dependent only on the experimental results. In addition, it is faster and cheaper than actual casting trials [26].

In investment casting, requested part geometries are generally quite complex, defect tolerances are quite limited, alloys such as titanium, superalloy, and ingot stainless steel are very expensive, ceramic shell coating ingredients are pricey and the process itself is time-consuming. Considering all these features, the development of a new product cycle consumes much time, and product cost increases in conjunction with the quantity of trial and amount of error. However, the emergence of simulation programs accelerates process optimization to shorten the new product development cycle and reduce the cost of the product and development [26].

Simulation software displays and allows for predicting filling, solidification processes, defect formation, and distribution of casting characteristics. Since the mid-1980s, numerical simulation software for flow and solidification of the casting process has become popular due to software and hardware developments. This numerical simulation software attracted the attention of casting company engineers and researchers. However, regarding statistical numbers, only 10-15% of all casting companies use casting simulation software tools in-house. The main reason behind this preference is to need for huge investment in this topic to integrate company datas into the software. To improve casting yield, minimize defects, obtain greater strength and fatigue performance, and ensure all customer requirements are met, most of casting companies have already started to use simulation-based casting methodology. This methodology includes computer-aided modeling of the casting part, casting tree design, casting method, process simulation, and optimization steps. According to the analysis of the entire casting process, it is obvious that simulation-based casting

technology is a more scientific proof-of-concept approach than the trial-and-error approach [27], [28].

Many casting simulation software tools have been developed with the help of physical phenomena occurring during casting. All these software are supported by mathematical models related to physical phenomena and a database of molten metals, mold materials, etc. Mold filling, solidification of molten metal and cooling of molten metal, and stress and strain profile of cast part are important features of casting simulations. Each feature has its equation. For instance, mold filling is based on continuity equation, momentum equation (Navier-Stokes), and energy equation. Solidification of molten metal is based on the solution of the energy equation. If fluid flow is not neglected, continuity and momentum equations shall be accounted for solidification. The stress-strain profile is based on equilibrium equations and Hooke's law [27], [29].

There are many simulation software used for casting processes such as AutoCAST, CAPCAST, CastCAE, MAGMASoft, ProCAST, FLOW-3D Cast, SOLIDCast, and Nova Flow & Solid. They are different from each other in terms of solution method, hardware requirement, user input, steps in simulation, and processing time. The subject of this thesis is based on Nova Flow & Solid simulation software which is used for high-pressure die casting, low-pressure die casting, gravity die casting, sand casting, centrifugal casting, lost foam casting, tilt pouring, and surely investment casting. There are also many solution methods. For instance, finite difference method, finite element method, vector element method, and finite volume method. Nova Flow & Solid uses the finite volume solution method. In Nova Flow & Solid material database involves a cast and ductile cast irons, plain and alloy steels, aluminum, copper, magnesium, and zinc alloys, and superalloys. Moreover, any casting alloy properties can be entered into the database. The user would like to see hot spots, riser effectiveness, chill effectiveness, insulation effectiveness, solidification direction, macro-solidification shrinkage, surface sink, microporosity, hydrogen porosity, hot tearing, final casting dimensions, casting distortion, residual stress, cold shuts, mold filling time, ingate effectiveness, runner effectiveness, pouring rate, post-pouring temperature distribution, turbulence, mold erosion, cold crack susceptibility, oxide film defects, lustrous carbon defects, bubble entrainment,

microstructure morphology, mechanical properties, grain size stray grains, freckling, and grain orientation. Nova Flow & Solid simulation software predicts the defects such as porosity, cold shuts, misruns, air entrapment, oxide skins, shrinkage, hot tearing and cracks, and thermal stress and interprets other required phenomenons using these results [27], [28].

All simulation software programs have comprehensive materials databases for molten metals, molds, and cores. These databases can be modified when required however, the reliability of simulation results depends on the accuracy of the simulation which is set by defining material properties, meshing, boundary conditions, etc.

So far, the thermophysical properties of ceramic shell molds have not been well documented. It is hoped that the results of this study may provide the researchers, who are willing to use simulation software computer programs, with necessary input parameters for their simulations

3. METHODOLOGY

3.1. Preparation of Samples

3.1.1. Material

The materials used in this study were prepared in the Gur Metal Investment Casting Company aluminum production line. Three different ceramic molds named A, B, and C were prepared by the aluminum casting line general application procedure. The molds differ from each other in terms of the slurries used for molding. Since the composition details are considered confidential information of the company they are not provided here. The information that can be given can be expressed as mold A was only shelled with primary slurry and zircon stucco, mold B was only shelled with backup slurry and zircon stucco, and mold C was shelled according to the general procedure in the aluminum production line, which includes both primary and backup slurries.

Shelling process details of ceramic mold samples are given in Table 3.1.

Table 3. 1 Shelling process details of ceramic mold samples.

Mold ID	Primary coat		Back-up coat		Seal coat	Dewaxing	Firing temp., ºC
	Slurry	Stucco	Slurry	Stucco	Slurry		
Mold A	Primary coat slurry	Zircon	N/A	N/A	Primary coat slurry	7 bar, 180ºC, 15 min.	6h, 800°C
Mold B	N/A	N/A	Back-up coat slurry (Colloidal Silica)	Zircon	Back-up coat slurry (Colloidal Silica)		
Mold C	Primary coat slurry	Zircon	Back-up coat slurry (Colloidal Silica)	Zircon	Back-up coat slurry (Colloidal Silica)		

Ceramic shell layer quantities and average ceramic mold wall thicknesses are given in Table 3.2.

Table 3. 2 Layer quantity and average ceramic mold wall thickness.

Mold ID	Ceramic Shell Layer Quantity	Average Ceramic Mold Wall Thickness (mm)
Mold A	5 + S	3.0915
Mold B	4 + S	4.0520
Mold C	6 + S	3.8805

Figure 3.1 shows the outer wall view of mold A.

Figure 3. 1 Outer wall view of mold A.

Figure 3.2 shows the inner wall view of mold A.

Figure 3. 2 Inner wall view of mold A.

Figure 3.3 shows the outer wall view of mold B.

Figure 3. 3 Outer wall view of mold B.

Figure 3.4 shows the inner wall view of mold B.

Figure 3. 4 Inner wall view of mold B.

Figure 3.5 shows the outer wall view of mold C.

Figure 3. 5 Outer wall view of mold C.

Figure 3.6 shows the inner wall view of mold C.

Figure 3. 6 Inner wall view of mold C.

3.1.2. Production of Investment Casting Ceramic Mold Samples

The samples used in the experimental studies were produced in a Turkish local investment casting company named Gur Metal Investment Casting. The flow that is shown in Figure 3.7 was followed for the production of samples.

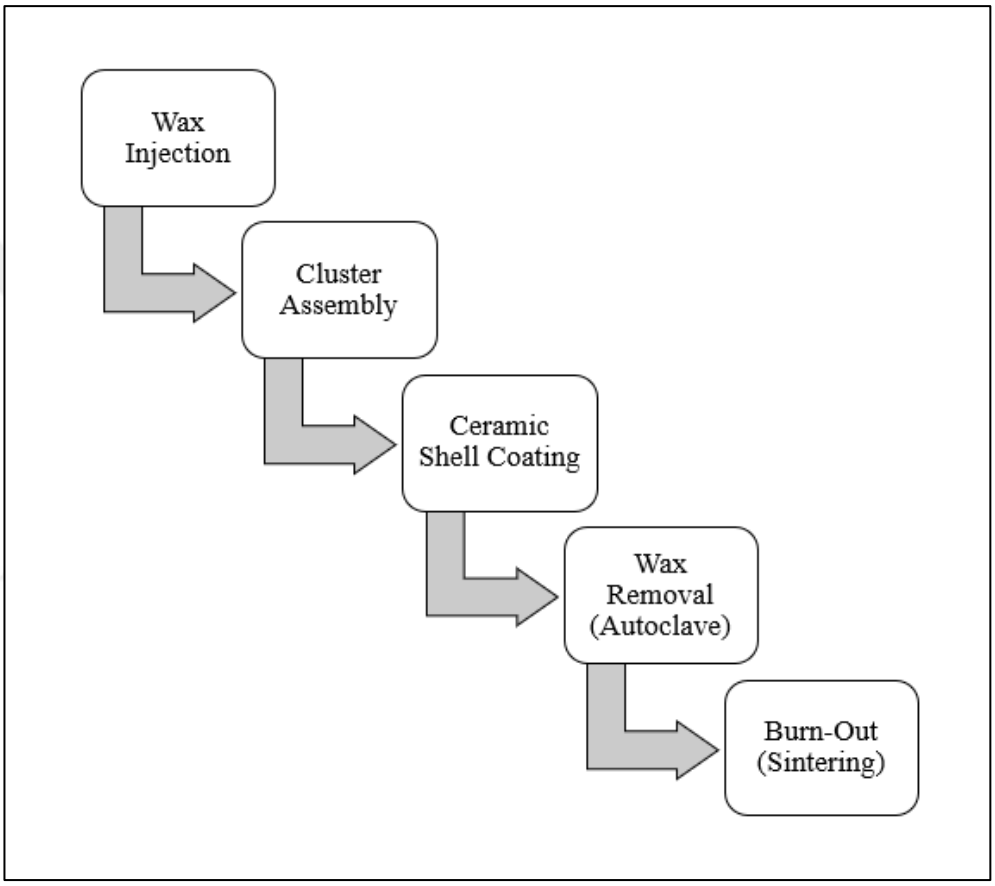

Figure 3. 7 Production flow of ceramic mold samples.

Brown wax samples with a thickness of 3.5 mm in the form of a 50 mm x 50 mm square were injected using an aluminum tool. The injection was carried out at 400 psi pressure and 65°C. Brown wax is preferred because of its general use in the aluminum production line. One day after the injection, 20 mm x 20 mm x 10 mm runners were stuck to one side of the samples as shown in Figure 3.8.

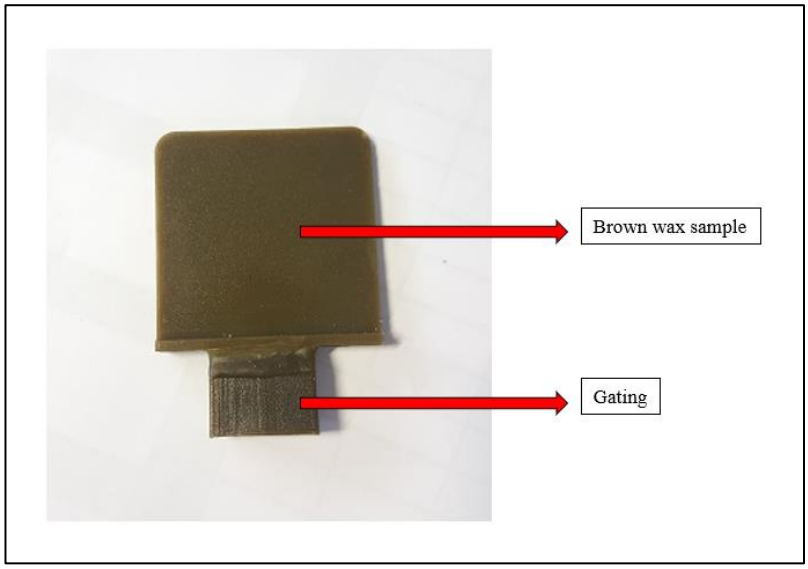

Figure 3. 8 Wax sample and gating.

After that, the casting tree was formed with 80 samples. Since three different ceramic molds were required for experimental studies, three casting trees were generated with the same methods. To distinguish the casting trees from each other and to ensure traceability, marking has been done.

To facilitate of the wax removal inside of the ceramic mold, four autoclave outlets were located on each casting tree as shown in Figure 3.9.

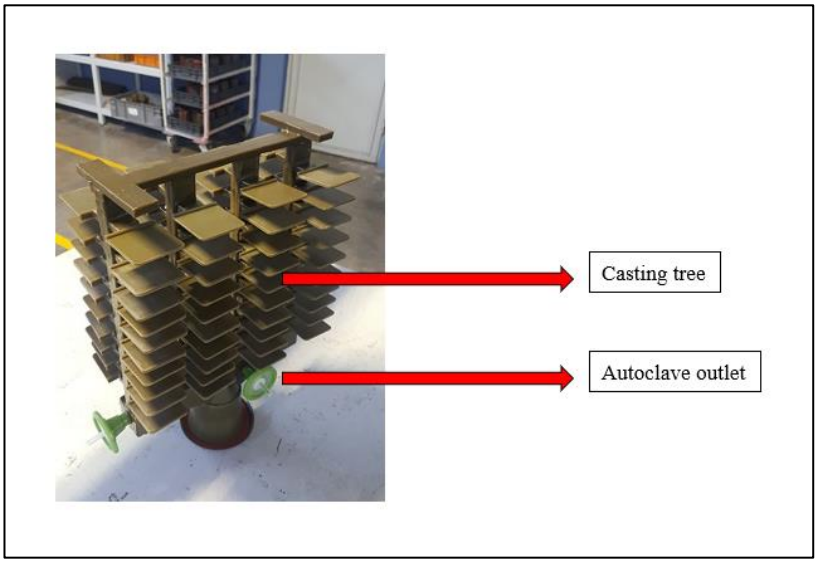

Figure 3. 9 Casting tree that involves 80 samples and 4 autoclave outlets.

Table 3. 3 Casting tree weights for each cluster.

Casting Tree	Mold Assignment	Casting Tree Weight (g)	Traceability of Casting Tree	Assigned Ceramic Mold Type
1st cluster	Mold A	2638	1 marking	Only primary coat
2nd cluster	Mold B	2702	2 markings	Only back-up coat
3rd cluster	Mold C	2732	3 markings	Standard application

Once the casting tree preparation was completed, the adhesive spray was sprayed around the cluster to ensure the ceramic slurries adhered to the wax surface. Each of the casting trees was sprayed with this adhesive spray. Figure 3.10 shows this adhesive spray and its application on the casting tree.

Figure 3. 10 Adhesive spray and its application.

After that, 1st cluster (mold A) was dipped into the primary coat slurry (see Figure 3.11).

Figure 3. 11 Dipping mold A into the primary slurry.

Then, it was powdered with zircon stucco (see Figure 3.12). This sequence was repeated until the ceramic shell thickness is reached to the max. 3.5 mm. The ceramic shell coating was ended when the shell thickness reached to avg. 3.0915 mm and this thickness was corresponded to 5 primary coats and 1 primary seal coat without zircon stucco.

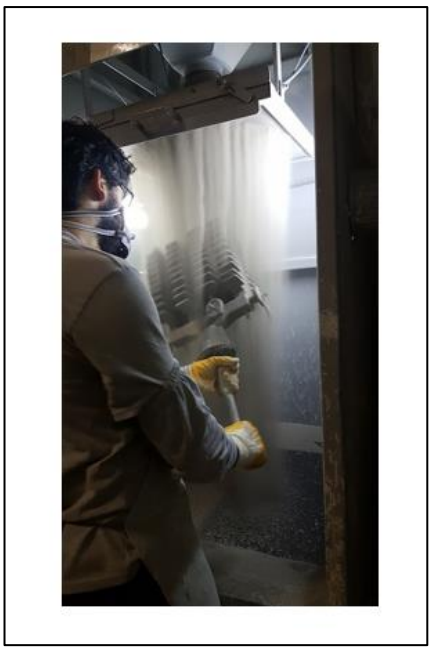

Figure 3. 12 Stuccoing of mold A with zircon sand.

When the casting tree was completely dried, the wax inside the tree was removed with the help of autoclave at 7 bar pressure, 180 ºC and in 15 minutes. Figure 3.13 shows appearance of a mold before and after wax removal.

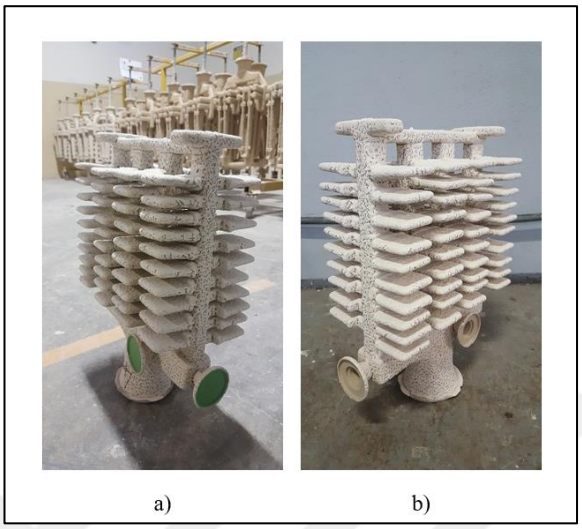

Figure 3. 13 Appearance of a mold a) before wax removal b) after wax removal.

After wax removal, the mold was burned-out 6 hours at 800 ℃ to remove green strength and give strenght to the mold.

Meanwhile, 2nd cluster (mold B) was dipped into the back-up coat slurry (see Figure 3.14).

Figure 3. 14 Dipping mold B into the back-up slurry.

Then, it was powdered with zircon stucco (see Figure 3.15). This sequence was repeated until the ceramic shell thickness reached to max. 3.5 mm. The ceramic shell coating was ended when the shell thickness was reached to avg. 4.0520 mm and this thickness corresponded to 4 back-up coats and 1 back-up seal coat without zircon stucco.

Figure 3. 15 Stuccoing of Mold B with zircon sand.

When the casting tree was completely dried, the wax inside of the tree was removed with the help of an autoclave at 7 bar pressure, 180ºC, and in 15 minutes.

After wax removal, the mold was burned-out for 6 hours at 800°C to remove green strength and give strength to the mold as applied for mold A.

Meanwhile, 3rd cluster (mold C) was dipped into the primary and back-up coat slurries as standard application procedure at Gur Metal Investment Casting aluminum production line (see Figure 3.16 and 3.17).

Figure 3. 16 Dipping mold C into the primary slurry.

Figure 3. 17 Dipping mold C into the intermediate slurry.

It was powdered with zircon stucco between each layer as applied for mold A and B (see Figure 3.18). This sequence was repeated until the ceramic shell thickness is reached to max. 3.5 mm. The ceramic shell coating was ended when the shell thickness was reached to avg. 3.8805 mm and this thickness was corresponded to 6 primary + back-up coats and 1 back-up seal coat without zircon stucco.

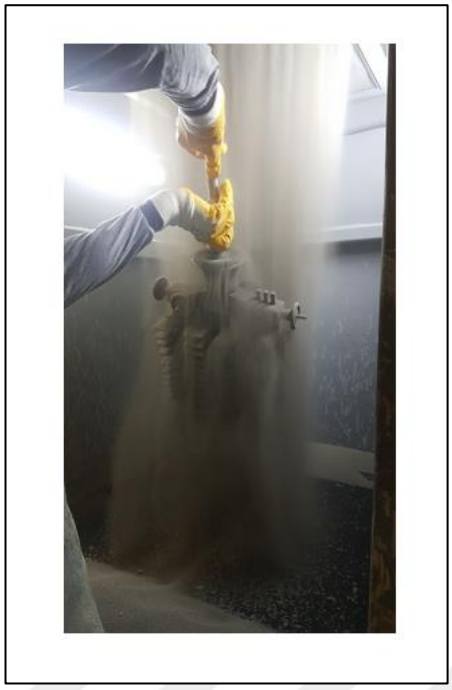

Figure 3. 18 Stuccoing with zircon sand.

When the casting tree was completely dried, the wax inside of the tree was removed with the help of autoclave at 7 bar pressure, 180ºC and in 15 minutes.

After wax removal, the mold was burned-out 6 hours at 800℃ to remove green strength and give strenght to the mold, using the same procedure as for molds A and B.

3.1.3. Preparation of Investment Casting Ceramic Mold Samples

Experimental studies were carried out with the samples produced in the aluminum production line of Gur Metal Investment Casting Company. The flow in Figure 3.19 was followed for the preparation of samples.

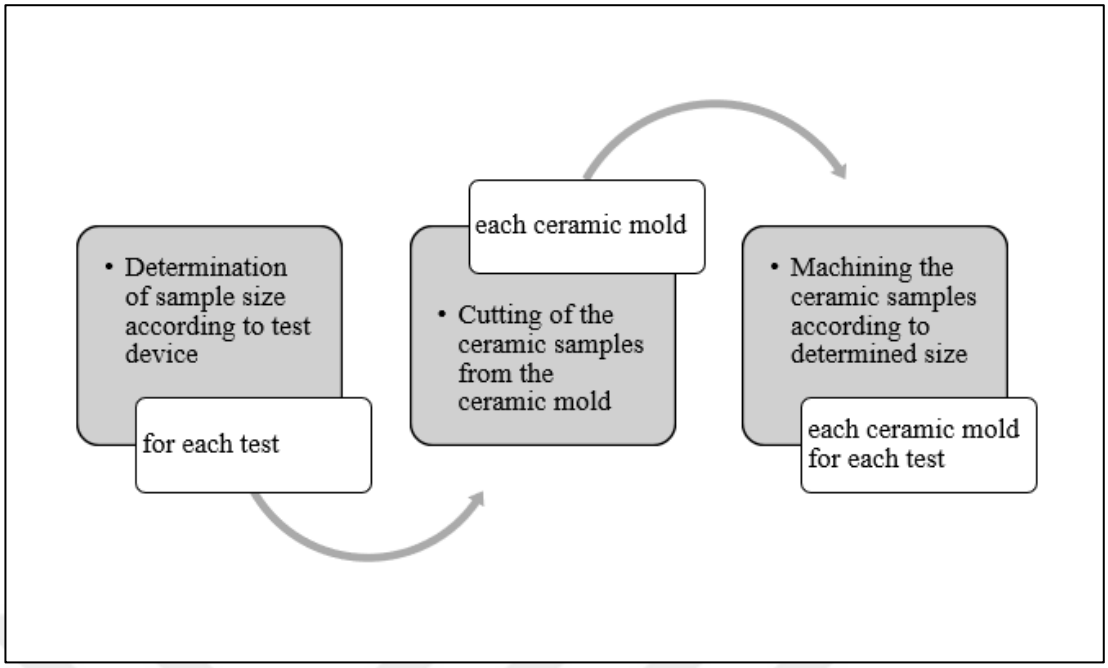

Figure 3. 19 Preparation flow of ceramic mold samples.

3.1.4. Determination of Specimen Size

Regarding to the literature search and the user manuals of the test devices, sample size for each test was determined. Table 3.4 shows required sample size of each test.

Table 3. 4 Sample dimensions based on test devices.

Test ID	**Required Sample Dimension (mm)**
Gas Permeability	L3.5 x Ø11
Specific Heat Capacity	L3.5 x Ø5.80
Density	L3.5 x Ø24

3.1.5. Separation of Samples from Ceramic Mold

Sintered square type ceramic samples were separated from ceramic mold with titanium saw blade using Makita angle grinder.

3.1.6. Machining of Ceramic Samples

Rough machining of ceramic samples were performed with a Ø10, Ø20 and Ø30 mm punches using Makita cordless drill. Precision machining of the samples were conducted using Struers LaboPol-5 Polisher and Struers RotoPol-11 Polisher. Machining was done in diameter only. The thickness was not. Changed.

3.2. Determination of Specific Heat

3.2.1. Experimental Procedure

The specific heats of the samples obtained from mold A, B and C were investigated with Differential Scanning Calorimetry (DSC) technique. DSC which is located in Characterisation Analysis Laboratory-1 of Aluminum Research and Application Center at Gebze Technical University (GTU) was used in this experimental study. For this purpose, Netzsch DSC 404 C (see Figure 3.25) was used to analyse specific heat's of the samples which representates A) only primary coat, B) only back-up coat C) aluminum production line general application procedure.

In this method mainly the samples were heated to the temperature that covers the interest of this experimental study at a controlled rate in a controlled atmopshere. During heating, the difference in heat flow on the samples and the reference material was observed and recorded.

Standard operating temperature interval of this device is from -120 to 1650°C. According to the design of experiment of this study, the ceramic mold samples were heated to 800°C with 10°C / minutes heating rate. The underlying cause of this design set is to study with Gur Metal Investment Casting aluminum production line and A356

casting aluminum alloy solidus liquidus temperature interval is ~ 572°C and ~ 610°C, respectively. Heating up to 800°C is quite enough to investigate specific heat of the samples. As a reference material 80 mg synthetic sapphire disk was used.

Since it is important for obtaining valid results, sample holder was used carefully. The samples were properly prepared according to the sample holder dimensions. Thus, the sample holder was completely filled and the most accurate results were expected. The Al_2O_3 crucible dimensions are indicated in Figure 3.20. Edges of the solid ceramic mold samples were polished with Struers LaboPol-5 Polisher (see Figure 3.21) to ensure that the samples are fit to this crucible. Water was not used during polishing because the samples were in fired condition.

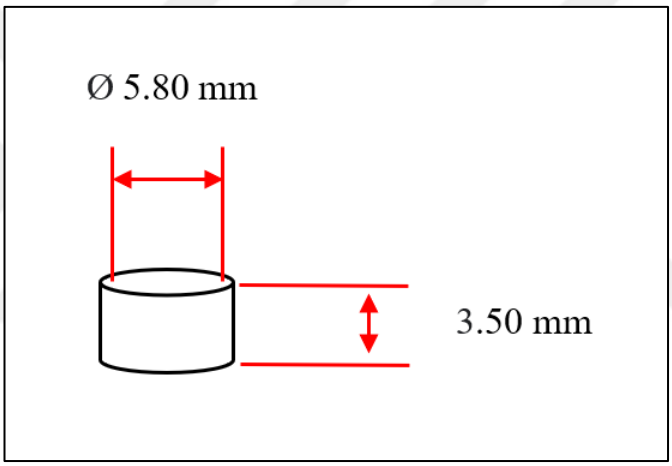

Figure 3. 20 Crucible dimensions of DSC.

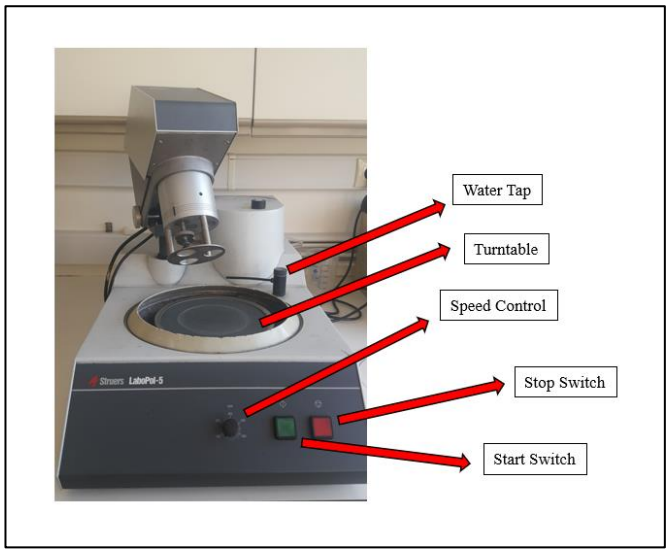

Figure 3. 21 Struers LaboPol-5 Polisher.

To see the repeatebility of this test results, three samples were prepared, and named X1, X2 and X3 for traceability. Figure 3.22, 3.23 and 3.24 show the mold A, B and C samples.

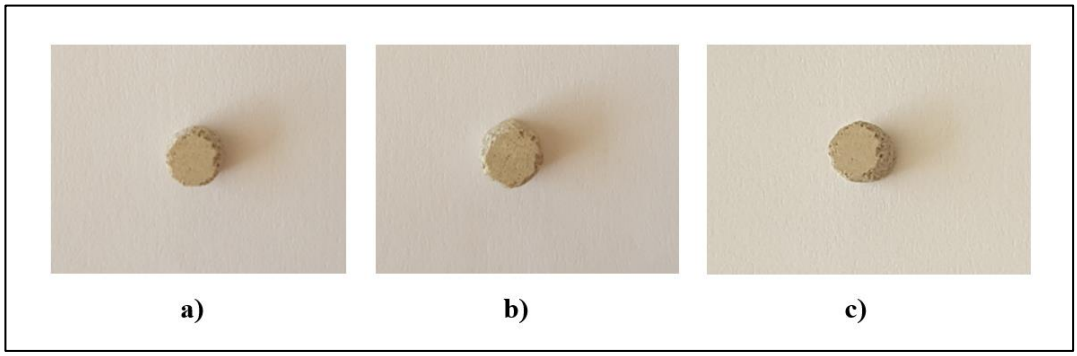

Figure 3. 22 Mold A samples a) A1 b) A2 c) A3.

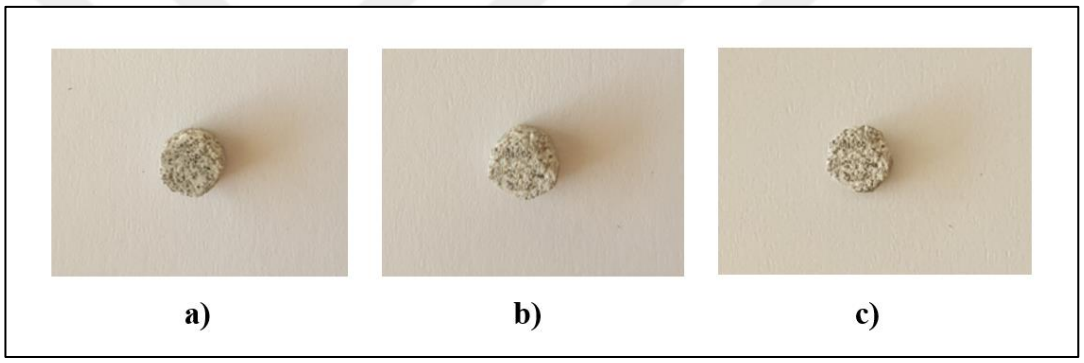

Figure 3. 23 Mold B samples a) B1 b) B2 c) B3.

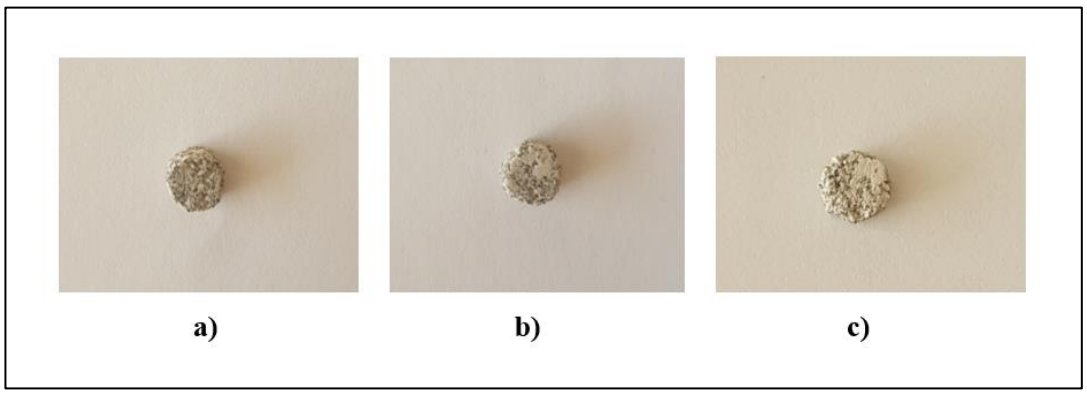

Figure 3. 24 Mold C samples a) C1 b) C2 c) C3.

Figure 3.26 shows Netzsch DSC 404 C.

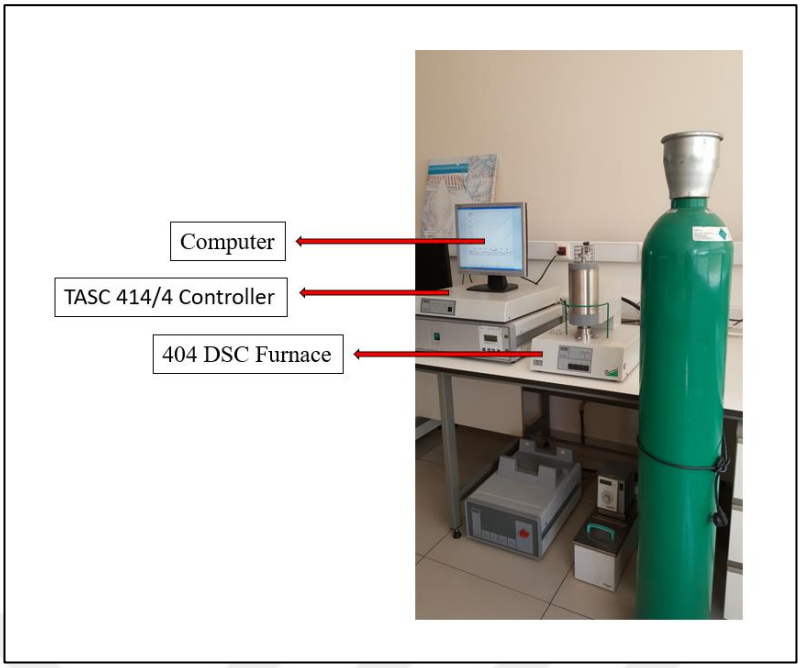

Figure 3. 25 Netzsch DSC 404 C.

3.3. Determinaation of Density

3.3.1. Experimental Procedure

The true densities of the samples obtained from mold A, B and C were investigated with Gas Pycnometer technique. Quantachrome Instrument, TM, model: Ultrapycnometer 1000 located in Mechanical Testing Laboratory at GTU (see Figure 3.32) was used and investigation was performed for mold representates A) only primary coat, B) only back-up coat C) aluminum production line general application procedure.

This method basically works based on fluid displacement revealed by Archimedes and the gas expansion expressed by Boyle's law. Helium gas was used for fluid displacement and easy penetration within the finest pores. It is used for this method and it assures maximum accuracy because it has small atomic dimensions and thus it is able to penetrate into even finest pores such as 0.2 nm in diameter [30] .

The samples were prepared for stainless steel sample holder conveniently. Figure 3.26 shows holder dimensions. Edges of the solid ceramic mold samples were

polished with Struers RotoPol-11 Polisher (see Figure 3.27) and became very fit to the holder. Polishing operation was completed without water since the samples were fired.

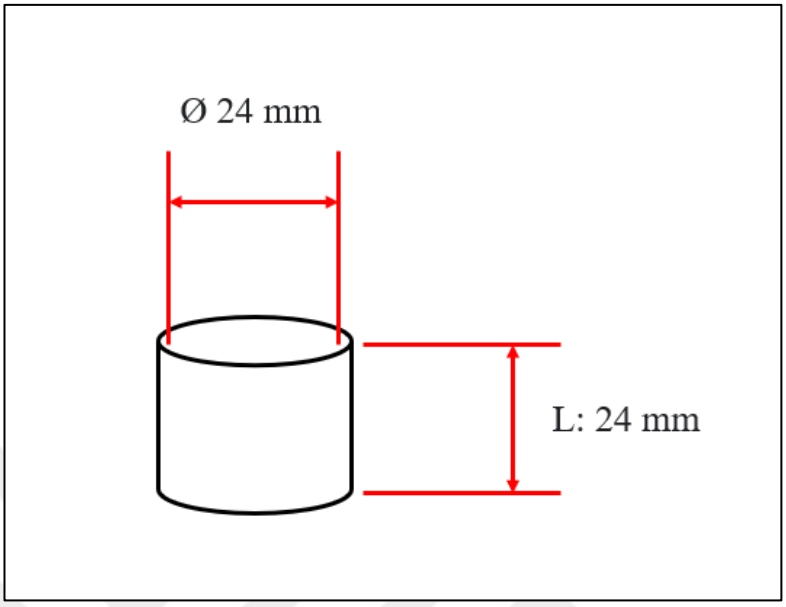

Figure 3. 26 Holder dimensions of gas-pycnometer.

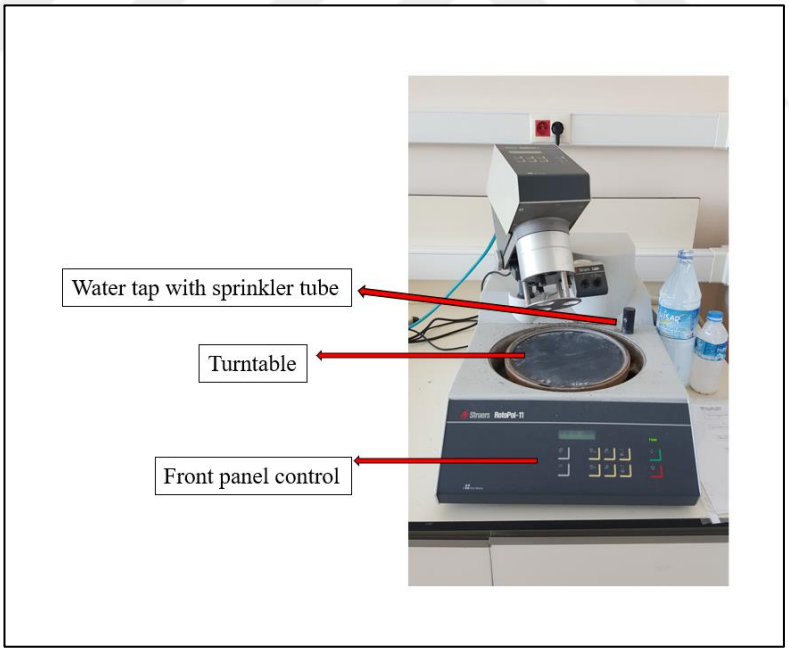

Figure 3. 27 Struers RotoPol-11 Polisher.

To see the repeatebility of this test results, three samples were prepared, and named X1, X2 and X3 for traceability. Figure 3.28, 3.29 and 3.30 show the mold A, B and C samples.

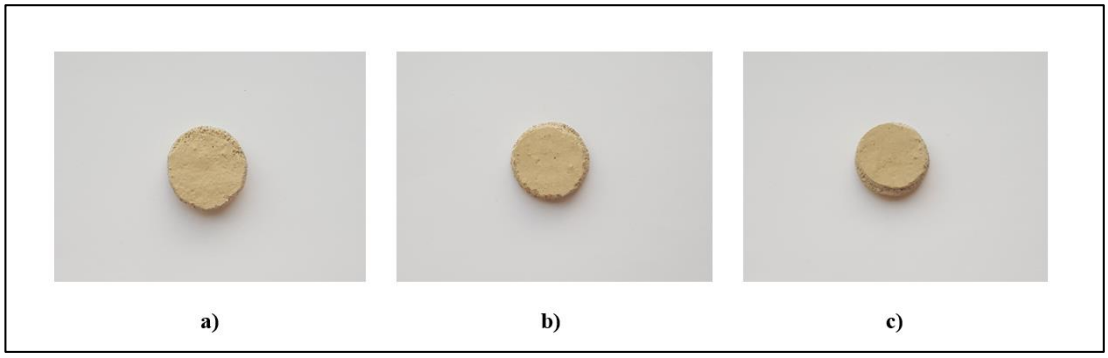

Figure 3. 28 Mold A samples a) A1 b) A2 c) A3.

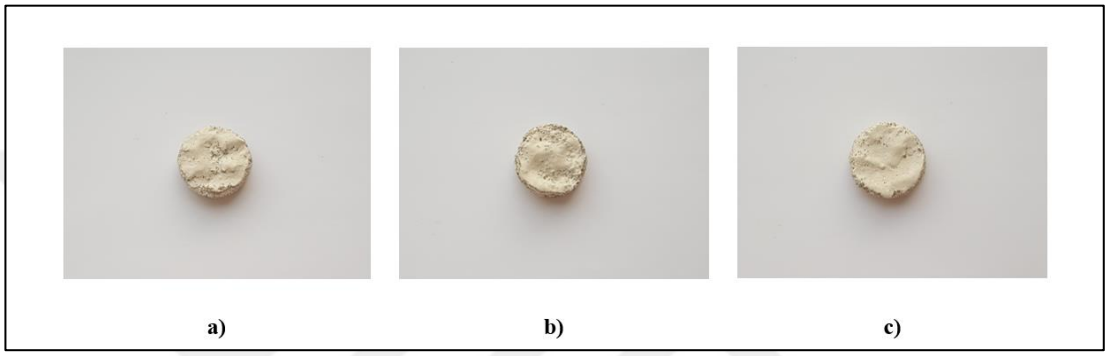

Figure 3. 29 Mold B samples a) B1 b) B2 c) B3.

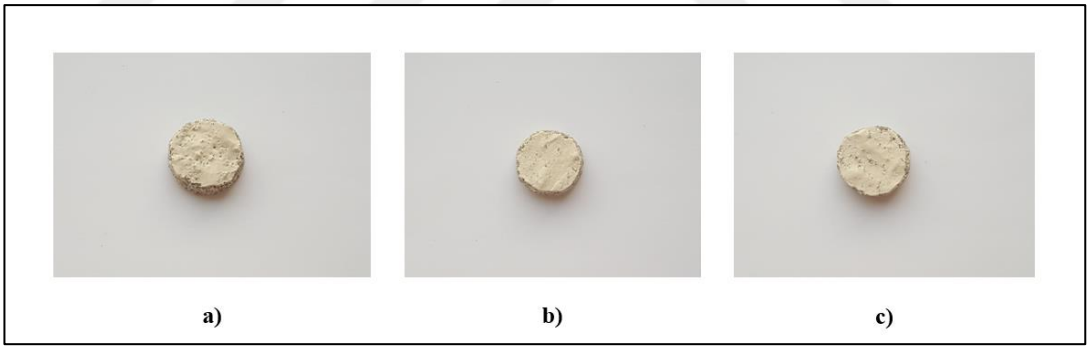

Figure 3. 30 Mold C samples a) C1 b) C2 c) C3.

Before start to test, the samples were weighed with Precisa XB 220A SCS Analytical Balance (see Figure 3.31) and noted. After that, these weight datas were fed into the pycnometer.

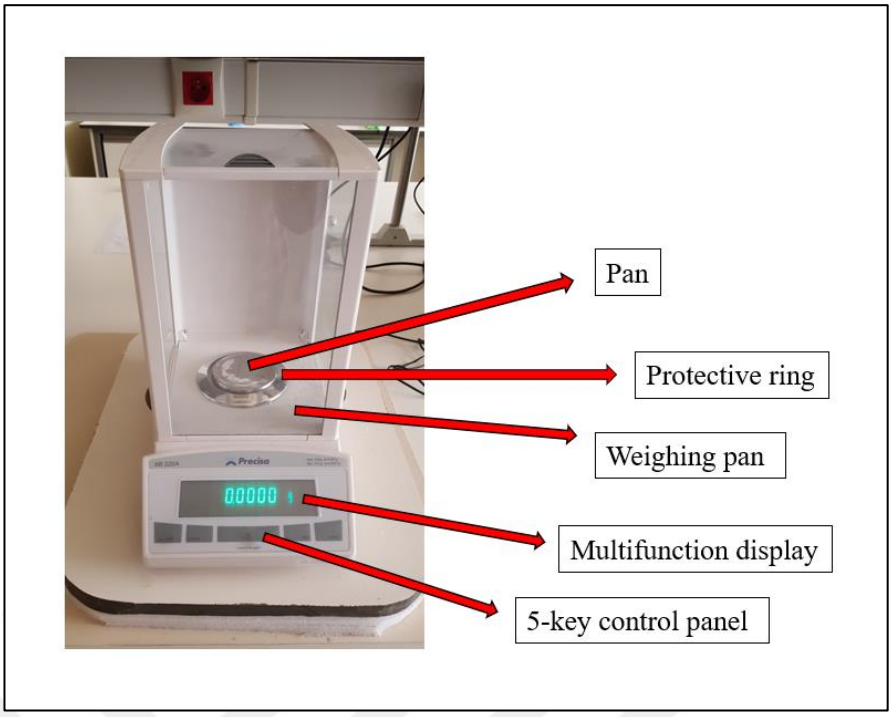

Figure 3. 31 Precisa XB 220A SCS Analytical Balance.

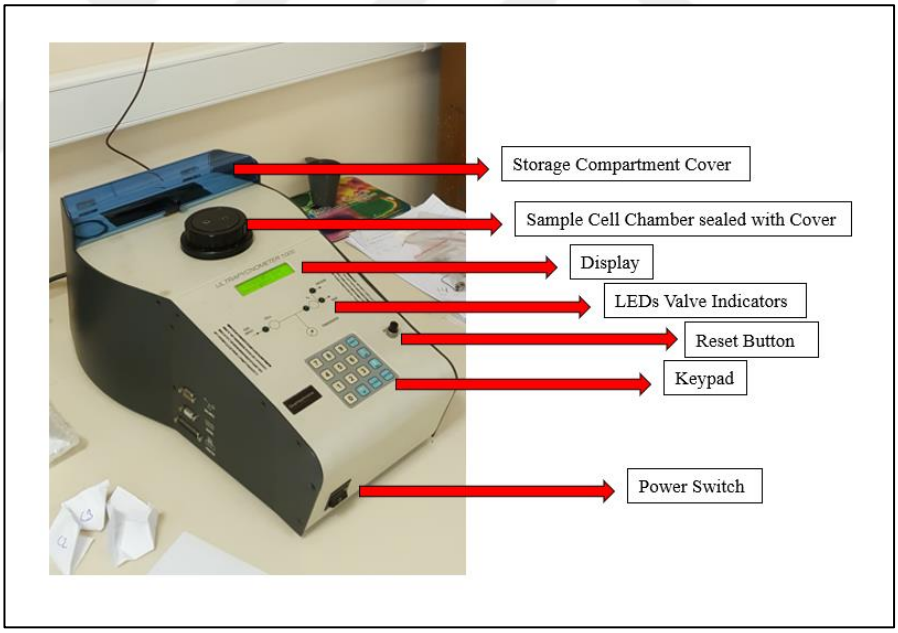

Figure 3. 32 Ultrapyc Controls And Connections.

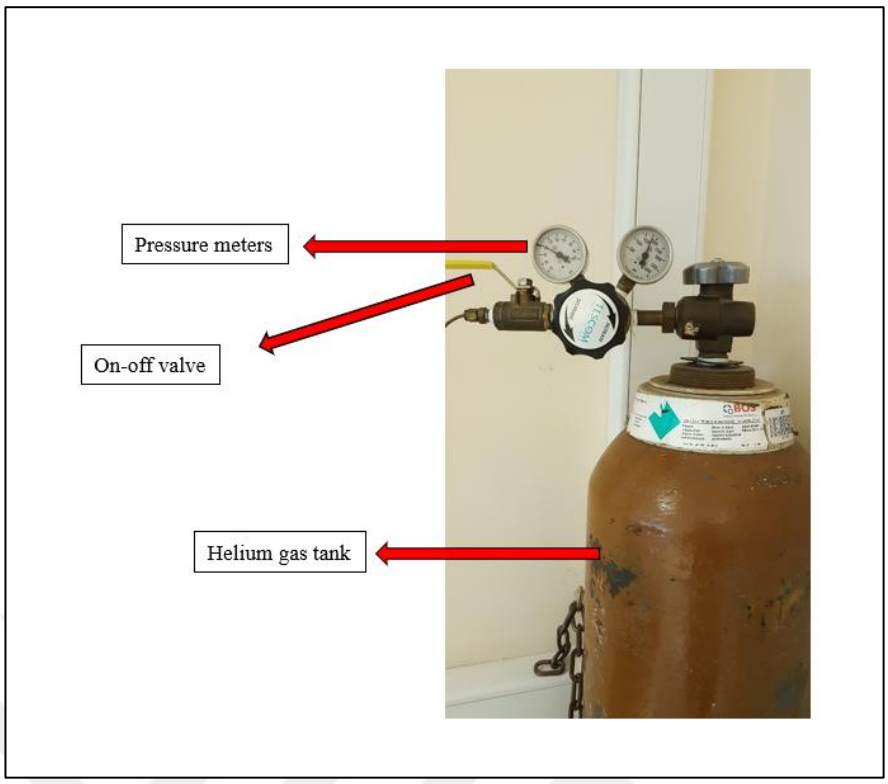

Figure 3. 33 Non-flammable and non-toxic gas.

3.4. Determination of Gas Permeability

3.4.1. Experimental Procedure

The gas permeability of the samples obtained from mold A, B and C were investigated with the in-house built set-up prepared in the Materials Physic Laboratory at GTU. For this experiment, nitrogen 5.0 gas tank, EN ISO 5171 certified nitrogen manometer, air 20ºC 101.3 Kpa 1.5 NL/min. flowmeter, hoses, lab retort stand and clamp holder were used. The results were recorded for each sample taken from Mold A) only primary coat, B) only back-up coat C) aluminum production line general application procedure.

This in-house built set-up was prepared according to ASTM C577-19 [31] Standard Test Method for Permeability of Refractories specification. However gas permeability calculation was conducted with two differents ways based on both ASTM [31] and another research for gas permeability studied by Zych et al. 2013 [32].

Obtained values from flowmeter and manometer during experiments were used for the calculation.

The approach in ASTM standard [31] is given by:

$$K = \frac{M\,Q\,L}{A\,\Delta P} \text{ x } 100 \qquad \textbf{Equation 3. 1}$$

where:

K = permeability, centidarcys,

M = gas viscosity, cP,

Q = flow rate, $\frac{cm^3}{s}$,

L = sample length, cm,

A = sample area, cm^2 , and

ΔP = absolute pressure drop across the sample, atm.

The approach in the reseacrh [32] is given by:

$$P_{reading} = \frac{V\,l}{A\,t\,p} \qquad \textbf{Equation 3. 2}$$

Where:

$P_{reading}$ = value read from the apparatus,

V = air volume passing through the sample (200 cm^3), m^3cm^3,

l = sample height (5 cm), m(cm),

A = surface of the sample cross-section (19,6 cm^2), m^2 (cm^2),

t = time, in which 200 cm^3 of air will pass through the sample s(min),

p = air pressure in the space under the sample (1 mm water column H_2O = 9,80665), $\frac{N}{m^2}$, Pa, ($\frac{G}{cm^2}$),

d = ceramic mould thickness (mm).

As seen from the Equaiton 3.1, ASTM calculation is based on centidarcys unit. However, Nova Flow&Solid casting solidification software requires the gas permeability value with different unit as located in the research done by Zych et al. 2013 [32]. The reason for this is that gas viscosity is also added to the formulation in

ASTM standard [31], however gas viscosity is not included in the research [32], just as Nova Flow & Solid expects. Both calculations were conducted and added to section 4.3.

The samples were prepared for Ø11 mm polymer hole sample holder conveniently. Figure 3.34 shows the holder dimensions. Edges of the solid ceramic mold samples were polished with Struers RotoPol-11 Polisher (see Figure 3.27) and became very fit to the holder. Polishing operation was completed without water since the samples were fired. Grease was applied around the samples to ensure sealing.

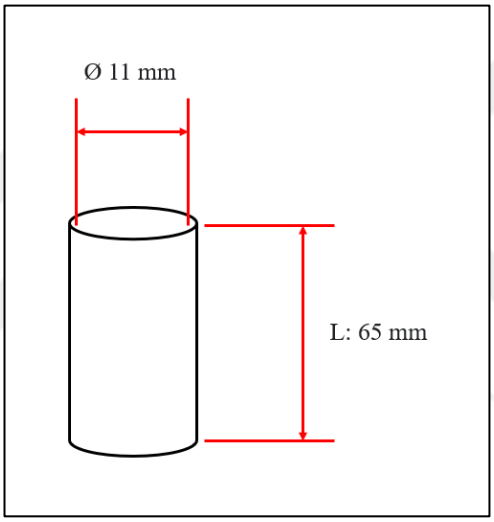

Figure 3. 34 Holder dimensions of gas permeability test set-up.

To see the repeatebility of this test results, three samples were prepared, and named X1, X2 and X3 for traceability. Figure 3.35, 3.36 and 3.37 show the mold A, B and C samples.

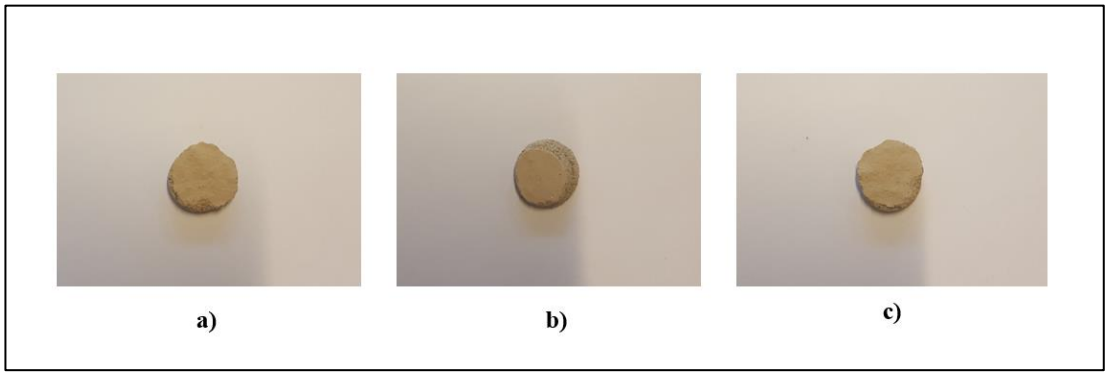

Figure 3. 35 Mold A samples a) A1 b) A2 c) A3.

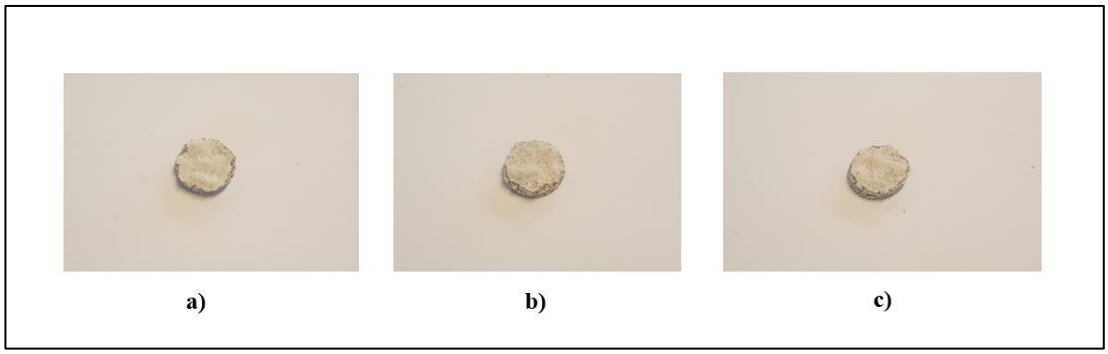

Figure 3. 36 Mold B samples a) B1 b) B2 c) B3.

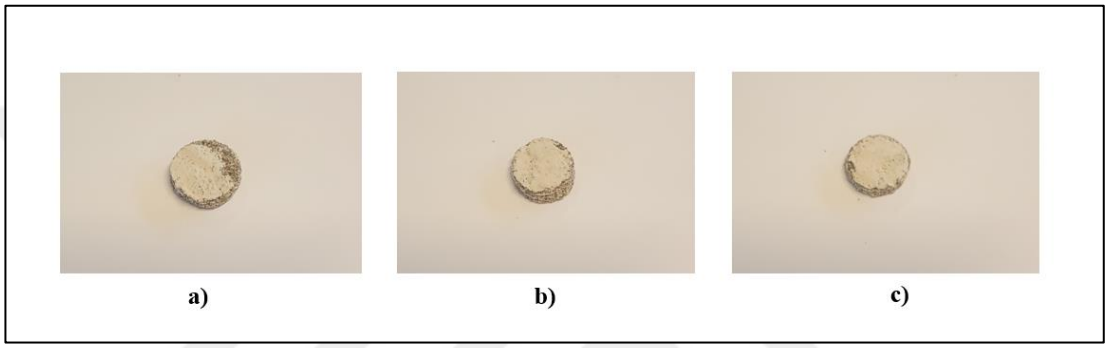

Figure 3. 37 Mold C samples a) C1 b) C2 c) C3.

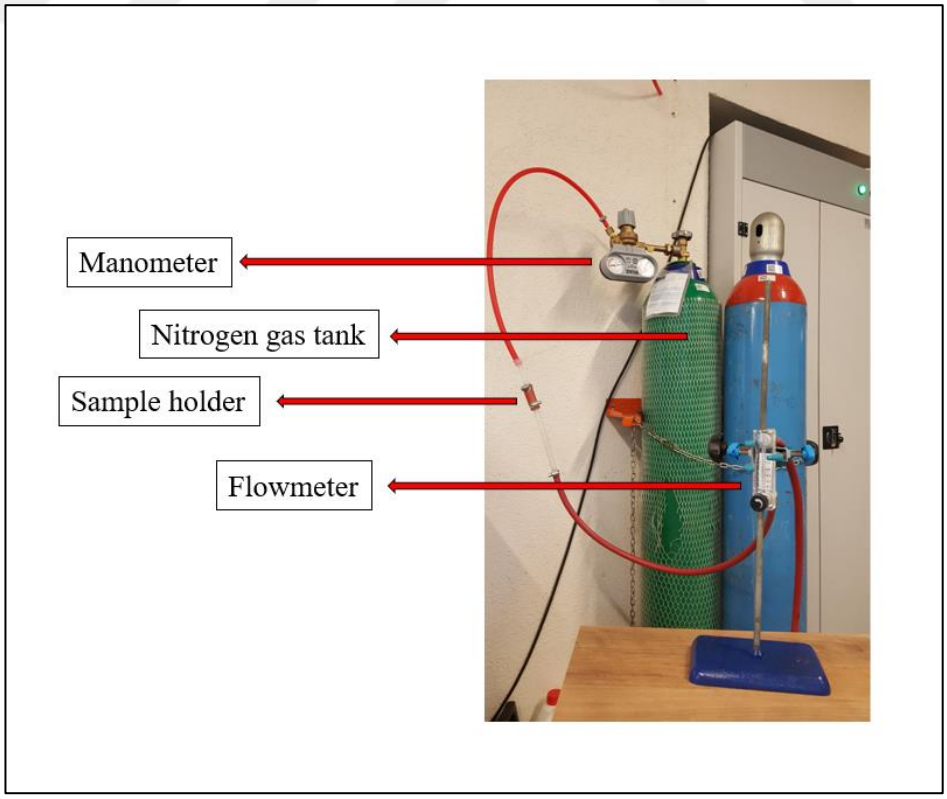

Figure 3. 38 In-house built gas permeability test set-up.

4. RESULTS

In order to investigate the thermophysical properties of the three different investment casting ceramic molds prepared in aluminum production line of Gur Metal Investment Casting Company, experimental studies were carried out with a total of nine samples.

The results of four experimental studies belong to each of the three molds were given in below chapters.

4.1. Specific Heat

4.1.1. Mold A Specific Heat Results

As of the molds were prepared in aluminum production line and the aluminum alloy used in this company was A356, the DSC analysis temperature was heated up to 800 ºC to cover the solidus-liqudus temperature of the alloy. The temperature rise rate is 10 ºC/min. and the measurement amount per min. is 40. With the placement and the removal of the sample, it took almost 2 hours per analysis.

The sapphire was used for the reference material and the each sample belongs to mold A was placed on the Al_2O_3 sample holder one by one.

Average results of the specific heat measurements of Mold A samples are given in Figure 4.1.

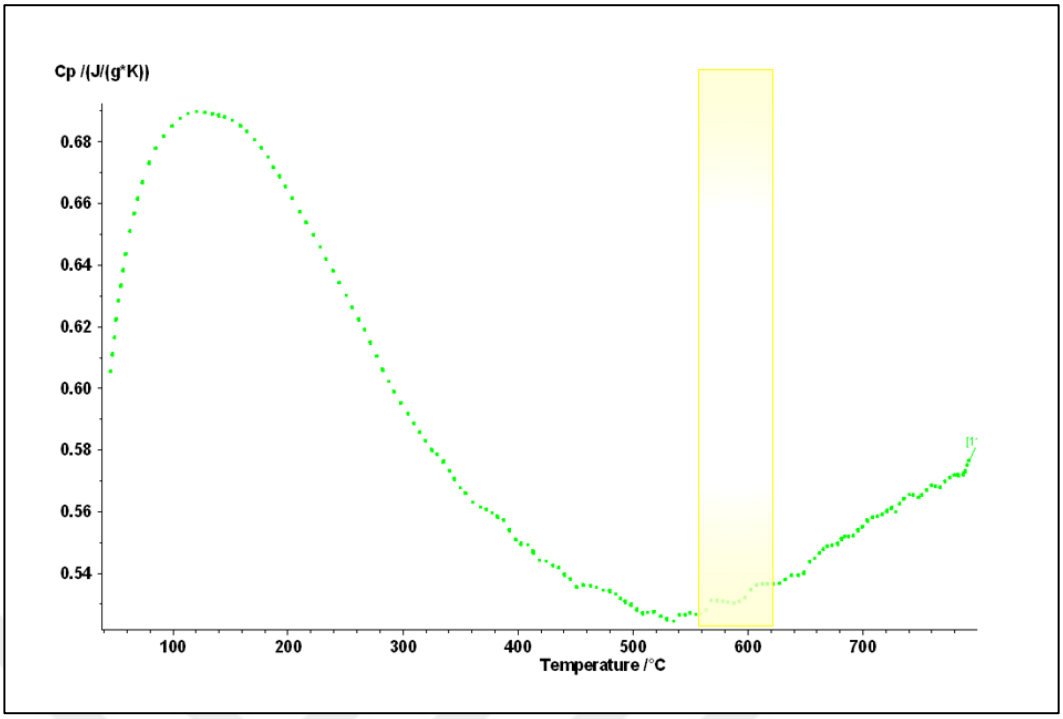

Figure 4. 1 Avg. specific heat values of mold A samples.

The green dots indicate the c_p values of the material at that temperature up to 800ºC. The highlighted region shows the temperature range subjected in this study. After the measurement was completed, the output of the device was taken in excel format. This output contains the c_p values per measuring point. In Table 4.1, the main measurement points and c_p values of the material in the temperature range of 572 - 610ºC are given. According to the results, the average c_p value between 572°C and 610°C is 0.5322 $\frac{J}{g\ K}$.

Table 4. 1 Mold A specific heat measurement results.

T, ºC	Time, min	Cp, $\frac{\mathbf{J}}{\mathbf{g\ K}}$
573	64.5	0.5312
575	64.7	0.5307
577	64.9	0.5313
579	65.1	0.5304
581	65.3	0.5312
583	65.5	0.5309
585	65.7	0.5303
587	65.9	0.5307

589	66.1	0.5304
591	66.3	0.5302
593	66.5	0.5308
595	66.7	0.5307
597	66.9	0.5315
599	67.1	0.5330
601	67.3	0.5339
603	67.5	0.5345
605	67.7	0.5358
607	67.9	0.5359
609	68.1	0.5363

4.1.2. Mold B Specific Heat Results

Since the mold prepared on the same production line with Mold A and Mold C and there should not be variation in parameters for comparable results, the DSC settings were kept the same for the specific heat measurements of Mold B.

Average results of the specific heat measurements of Mold B samples are given in Figure 4.2.

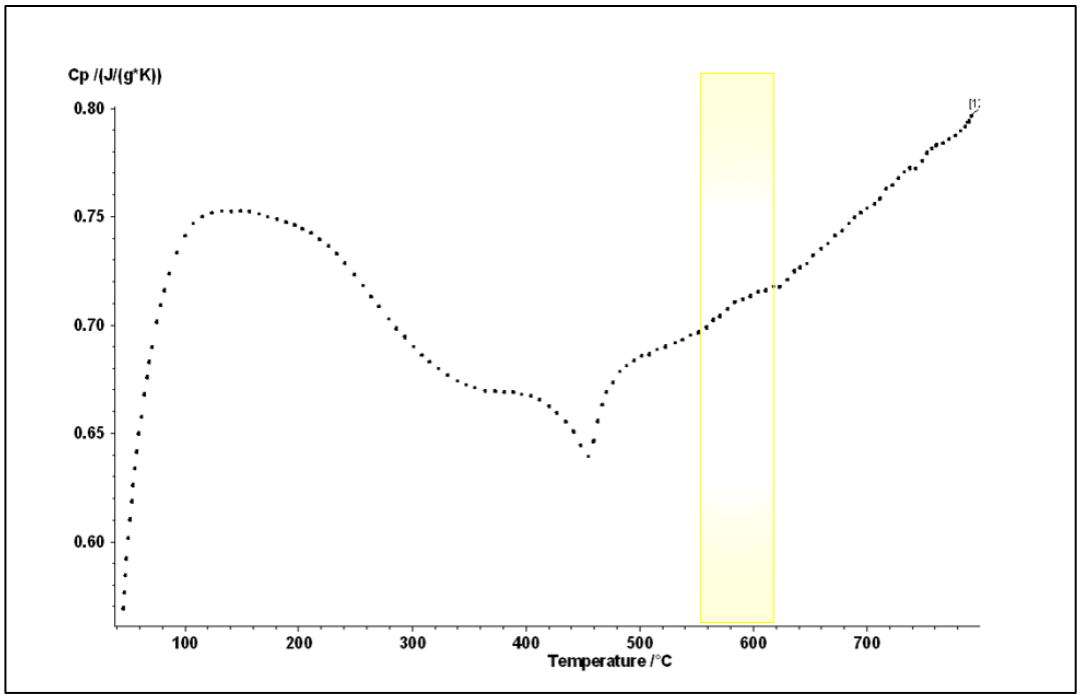

Figure 4. 2 Avg. specific heat values of mold B samples.

This time, the black dots show the c_p values of the material at that temperature. The highlighted region indicates the temperature interval subjected in this study as 572°C to 610°C. The prinout of the device was taken and the main numerical results are given in Table 4.2. The average c_p value between 572°C and 610°C is 0.7119 $\frac{J}{g\,K}$.

Table 4. 2 Mold B specific heat measurement results.

T, °C	**Time, min**	**Cp, $\frac{\mathbf{J}}{\mathbf{g\,K}}$**
573	64.5	0.7052
575	64.7	0.7065
578	64.9	0.7076
580	65.3	0.7092
583	65.5	0.7099
585	65.7	0.71
588	65.9	0.7114
590	66.3	0.7117
593	66.5	0.7126
595	66.7	0.7133
598	66.9	0.7138
600	67.3	0.7149
603	67.5	0.7147
605	67.7	0.7161
608	68.1	0.7167
610	68.3	0.7162

4.1.3. Mold C Specific Heat Results

The same analysis procedures applied for Mold A and Mold B were implemented and the same DSC settings were kept for the specific heat measurements of Mold C.

Average results of the specific heat measurements of Mold C samples are given in Figure 4.3.

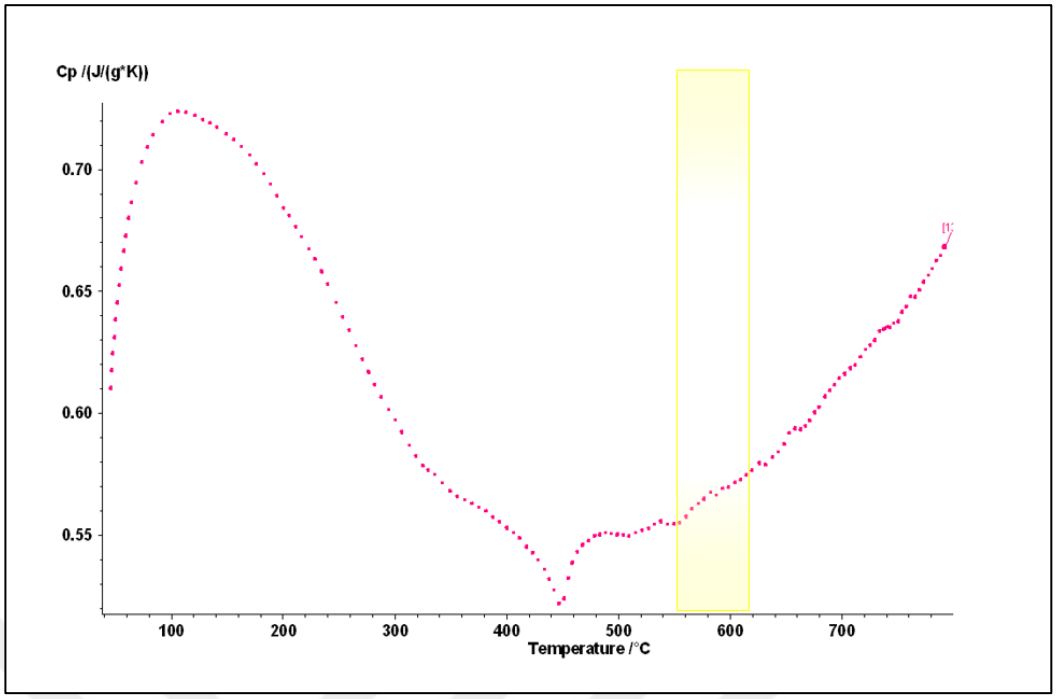

Figure 4. 3 Avg. specific heat values of mold C samples.

The pink points show the c_p values of the material at each that temperature up to 800ºC. The highlighted region indicates the solidus-liquidus temperature range of A356 aluminum alloy, and these are the temperatures for the purpose of this research. The main results of the measurements taken from the excel output of the device are given in Table 4.3. The average c_p value between 572°C and 610°C is 0.7105 $\frac{J}{g\,K}$.

Table 4. 3 Mold C specific heat measurement results.

T, ºC	Time, min	Cp, $\frac{\mathbf{J}}{\mathbf{g\,K}}$
572	64.5	0.5629
575	64.7	0.5638
577	64.9	0.5656
580	65.3	0.5670
582	65.5	0.5674
585	65.7	0.5668
587	65.9	0.5664
590	66.3	0.5679
592	66.5	0.5689

595	66.7	0.5692
597	66.9	0.5697
600	67.3	0.5708
602	67.5	0.5716
605	67.7	0.5722
607	67.9	0.5725
610	68.3	0.5728

4.2. Density

Before starting to measure the true densities with Ultrapycnometer 1000 gas pycnometer (see Figure 3.32), the samples were weighed with Precisa XB 220A SCS Analytical Balance (see Figure 3.31) and the results recorded. Using these values, the bulk volumes of each sample were calculated with the following mathematical formula.

$$\text{Volume} = l\ w\ h \qquad \textbf{Equation 4. 1}$$

Where;

l = length,
w = width,
h = height.

Then, the bulk densities of each sample were calculated with the following mathematical formula.

$$d = \frac{m}{v} \qquad \textbf{Equation 4. 2}$$

Where;

d = density,
m = mass,
v = volume.

After all, the true densities of the samples of each mold were analyzed by gas pycnometer.

4.2.1. Mold A Density Results

The bulk data obtained from Mold A samples are given in Table 4.4.

Table 4. 4 Bulk volume and density values of Mold A Samples.

Sample ID	Weight (g)	Bulk Volume (mm^3)	Bulk Density ($\frac{g}{cm^3}$)	Avg. Density ($\frac{g}{cm^3}$)
A1	1.3415	890.19	1.5070	1.5482
A2	1.2638	890.19	1.4197	
A3	1.5292	890.19	1.7178	

The true weight values were fed to the device and the true densities were calculated with the gas-pycnometer. The true densities calculated by the device are given in Table 4.5.

Table 4. 5 True volume and density values of Mold A Samples.

Sample ID	Weight (g)	True Volume (mm^3)	True Density ($\frac{g}{cm^3}$)	Avg. Density ($\frac{g}{cm^3}$)
A1	1.3415	424.8	3.1580	2.8116
A2	1.2638	528.9	2.3893	
A3	1.5292	529.6	2.8874	

4.2.2. Mold B Density Results

The bulk data calculated using Equation 4.1 and 4.2 for Mold B samples are given in Table 4.6.

Table 4. 6 Bulk volume and density values of Mold B Samples.

Sample ID	Weight (g)	Bulk Volume (mm^3)	Bulk Density ($\frac{g}{cm^3}$)	Avg. Density ($\frac{g}{cm^3}$)
B1	1.5744	890.19	1.7686	1.7787
B2	1.6114	890.19	1.8102	
B3	1.5642	890.19	1.7572	

The true weight values were entered into the device and the true densities were calculated with the gas-pycnometer as already performed for Mold A samples. The true densities calculated by the device are given in Table 4.7.

Table 4. 7 True volume and density values of Mold B Samples.

Sample ID	Weight *(g)*	True Volume *(mm^3)*	True Density ($\frac{g}{cm^3}$)	Avg. Density ($\frac{g}{cm^3}$)
B1	1.5744	575.2	2.7372	2.7348
B2	1.6114	592.8	2.7184	
B3	1.5642	569.0	2.7488	

4.2.3. Mold C Density Results

The same equations (Equation 4.1 and 4.2) used to calculate bulk data of Mold C samples. They are given in Table 4.8.

Table 4. 8 Bulk volume and density values of Mold C Samples.

Sample ID	Weight (g)	Bulk Volume (mm^3)	Bulk Density ($\frac{g}{cm^3}$)	Avg. Density ($\frac{g}{cm^3}$)
C1	1.3793	890.19	1.5494	1.5398
C2	1.3762	890.19	1.5460	
C3	1.3567	890.19	1.5241	

The true densities calculated by the gas pycnometer are given in Table 4.9.

Table 4. 9 True volume and density values of Mold C Samples.

Sample ID	**Weight (g)**	**True Volume (mm^3)**	**True Density ($\frac{g}{cm^3}$)**	**Avg. Density ($\frac{g}{cm^3}$)**
C1	1.3793	506.1	2.7256	2.7343
C2	1.3762	506.1	2.7195	
C3	1.3567	491.9	2.7579	

4.3. Gas Permeability

The gas permeability analysis was conducted with an in-house built set-up at room temperature. The analysis took long 20 min. per sample including gas permeability measurement and sample placement to the holder of the set-up. After the experiment was completed, gas permeability values were calculated based on the two equations as 3.1 and 3.2. Equation 3.1 was taken from ASTM C577-19 [31] standard and Equation 3.2 was taken from another study by Zych et al. 2013 [32]. The difference between these results is the unit since the formulas require different parameters which concludes the calculation with different units. The gas permeability value desired to be achieved in this study is met by the results calculated with the Equation 3.2.

4.3.1. Mold A Gas Permeability Results

The gas permeability measurement results of Mold A samples which were obtained by using Equation 3.1 are given in Figure 4.4.

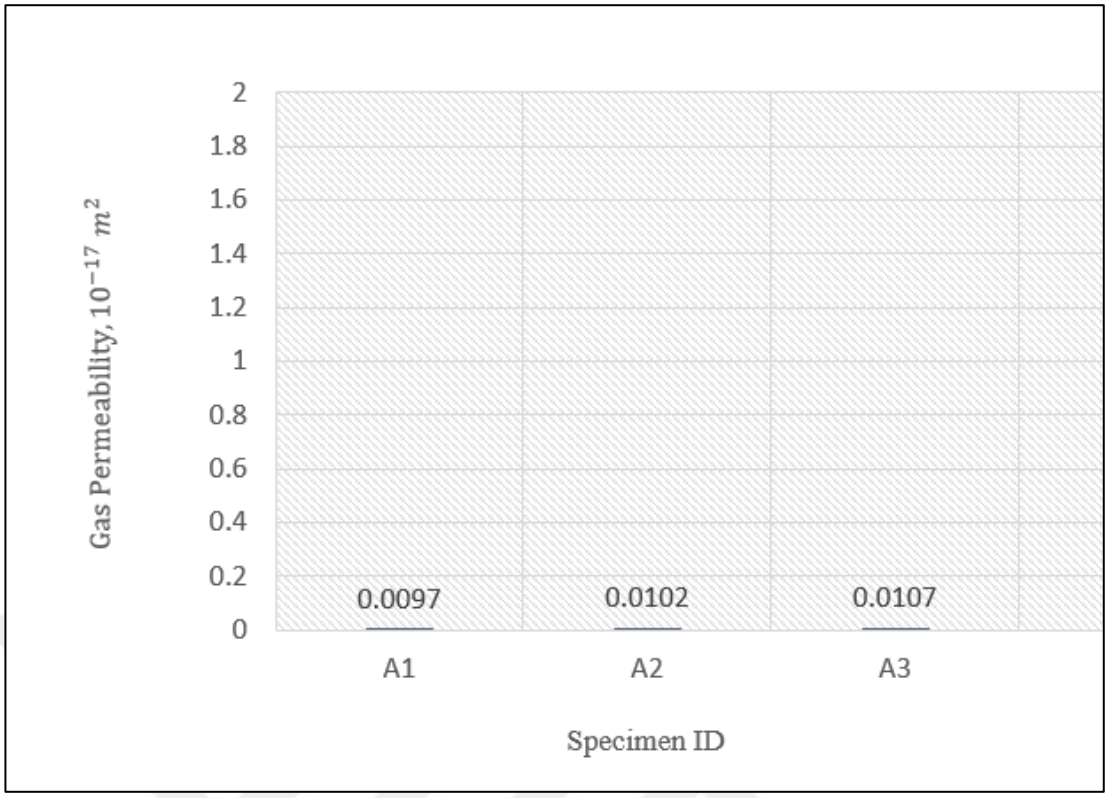

Figure 4. 4 Gas permeability values of Mold A samples based on Equation 3.1.

The average gas permeability value of Mold A samples based on Equation 3.1 is 1.0102 x 10^{-17} m^2.

The gas permeability measurement results of Mold A samples which were obtained by using Equation 3.2 are given in Figure 4.5.

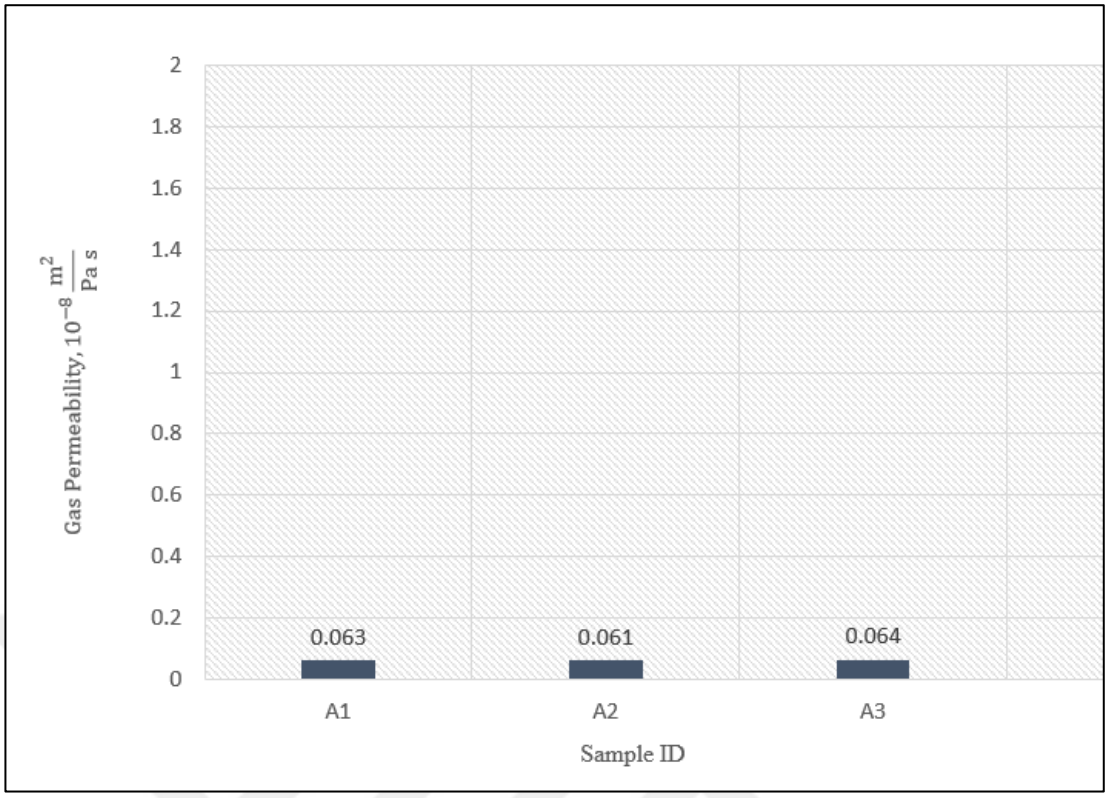

Figure 4. 5 Gas permeability values of Mold A samples based on Equation 3.2.

The average gas permeability value of Mold A samples based on Equation 3.2 is 0.063 x $10^{-8}\ \frac{m^2}{Pa\ s}$.

4.3.2. Mold B Gas Permeability Results

The gas permeability measurement results of Mold B samples based on Equation 3.1 are given in Figure 4.6.

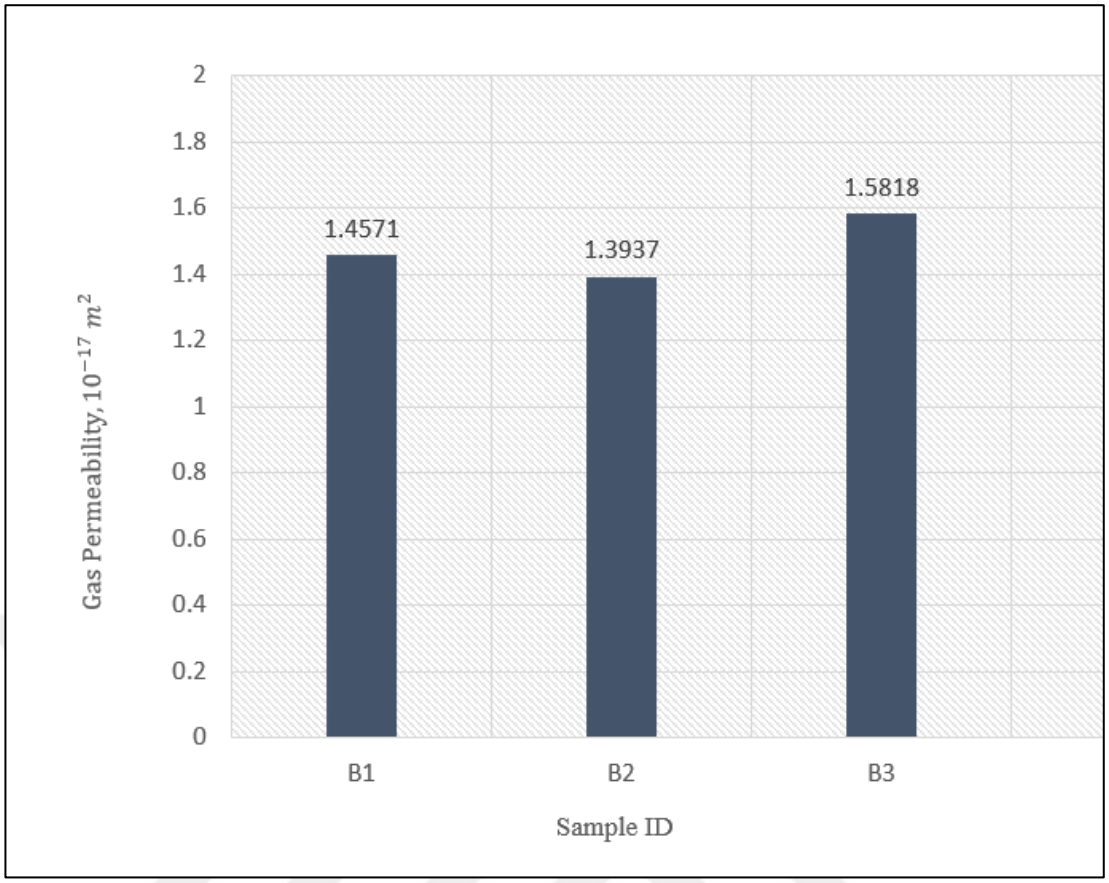

Figure 4. 6 Gas permeability values of Mold B samples based on Equation 3.1.

The average gas permeability value of Mold B samples based on Equation 3.1 is 1.4776 x 10^{-17} x m^2.

The gas permeability measurement results of Mold B samples based on Equation 3.2 are given in Figure 4.7.

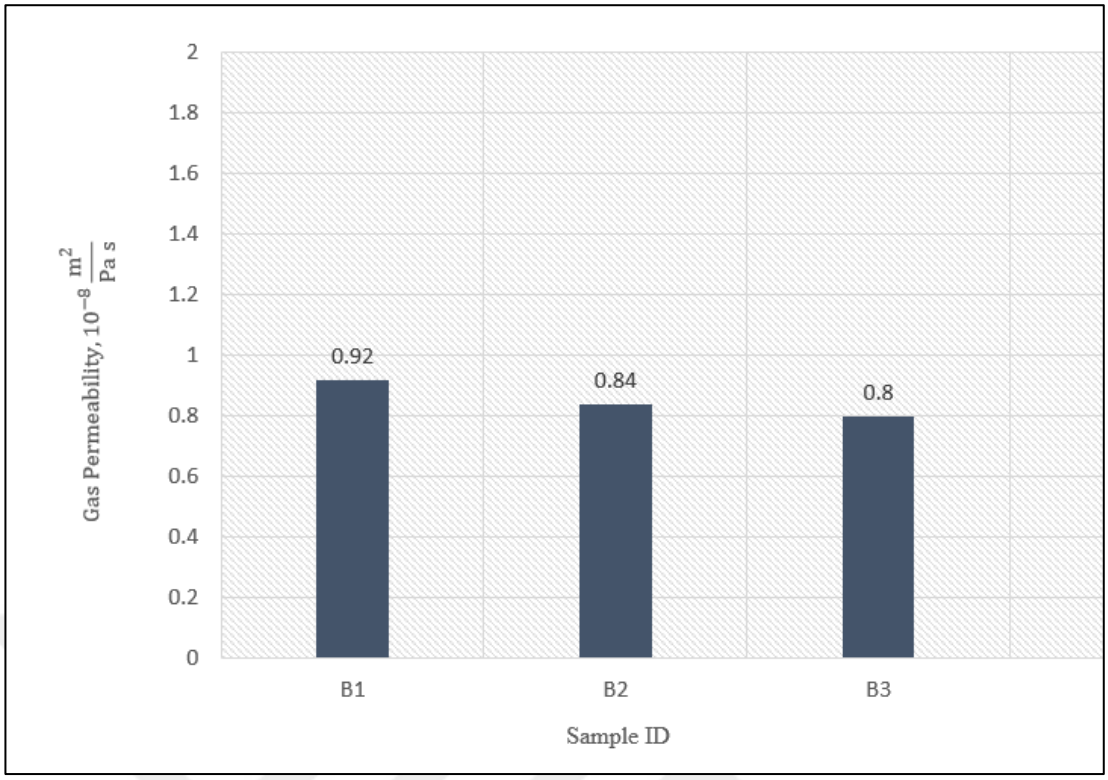

Figure 4. 7 Gas permeability values of Mold B samples based on Equation 3.2.

The average gas permeability value of Mold B samples based on Equation 3.2 is 0.85 x $10^{-8}\frac{m^2}{Pa\ s}$.

4.3.3. Mold C Gas Permeability Results

The gas permeability measurement results of Mold C samples are given in Figure 4.8.

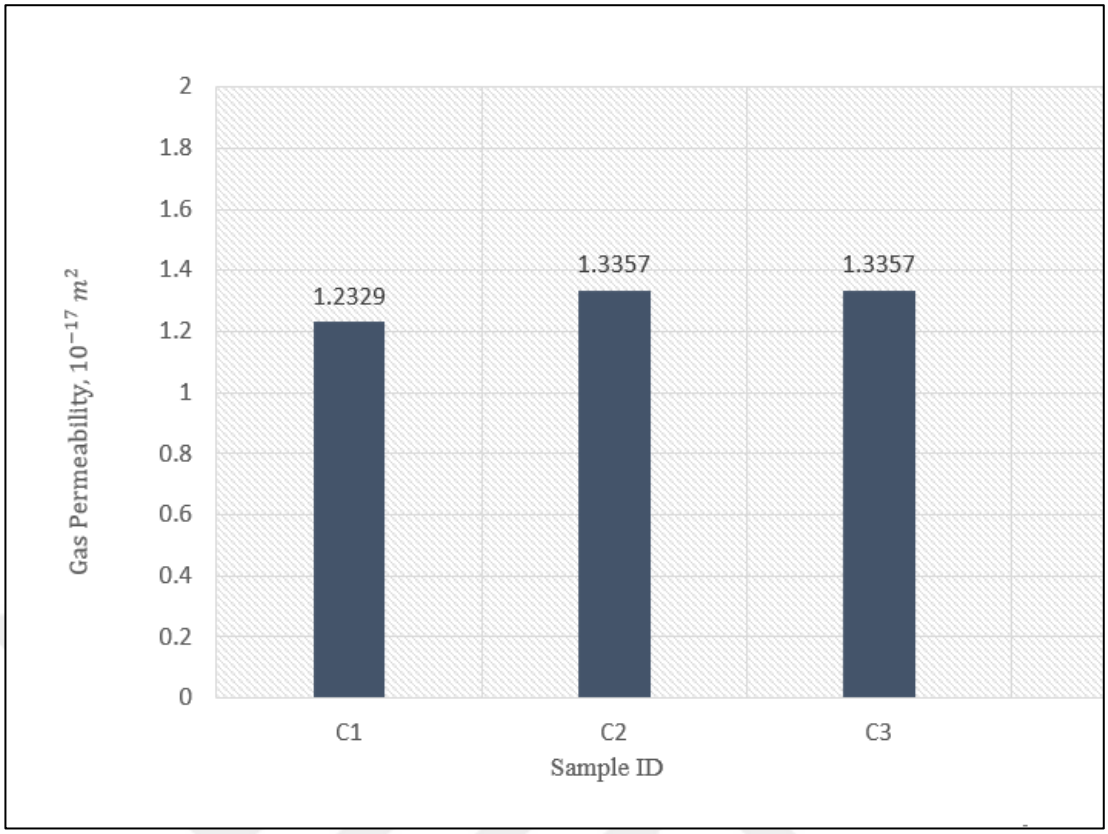

Figure 4. 8 Gas permeability values of Mold C samples based on Equation 3.1.

The average gas permeability value of Mold C samples based on Equation 3.1 is 1.3014 x 10^{-17} x m^2.

The gas permeability measurement results of Mold C samples based on Equation 3.2 are given in Figure 4.9.

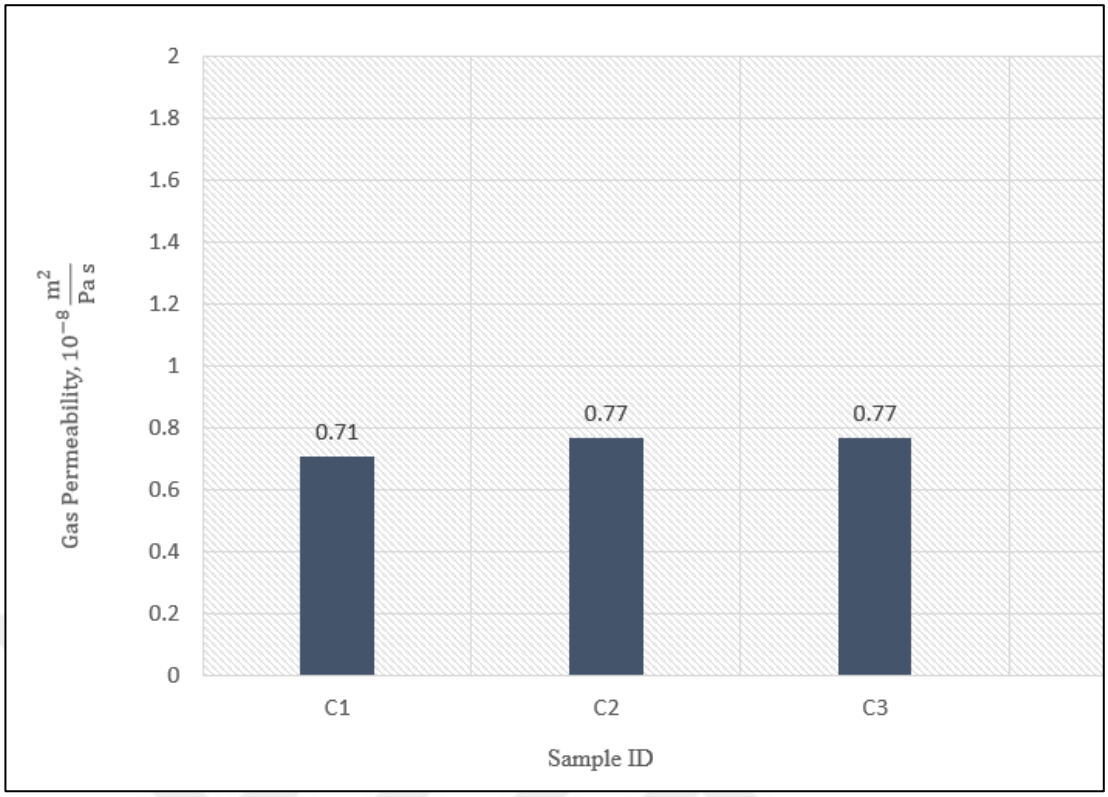

Figure 4. 9 Gas permeability values of Mold C samples

The average gas permeability value of Mold A samples is 0.75 x 10^{-8} $\frac{m^2}{Pa\,s}$.

5. DISCUSSION

In order to investigate the thermophysical properties of ceramic molds produced at Gur Metal Investment Casting Company, the experimental studies were carried out with 3 molds prepared with different slurry combinations. Among the 3 molds only Mold C represents the actual mold used for casting in Gur Metal. The other molds were prepared only to symbolise the primary and back-up layer features. The experiment matrix is given in Table 5.1 and 5.2.

Table 5.1 shows the material information used in the experiments and Table 5.2 shows the tests carried out for these materials.

Table 5. 1 Matrix of materials used in experimental studies.

Coat ID / Mold ID	Primary Coat		Back-up Coat		Seal Coat
	Slurry	**Stucco**	**Slurry**	**Stucco**	**Slurry**
Mold A	Primary coat slurry	Zircon	N/A	N/A	Primary coat slurry
Mold B	N/A	N/A	Colloidal Silica	Zircon	Colloidal Silica
Mold C	Primary coat slurry	Zircon	Colloidal Silica	Zircon	Colloidal Silica

Table 5. 2 Matrix of analysis objected in experimental studies.

Analysis ID / Mold ID	Specific Heat	Density	Gas Permeability
Mold A	✓	✓	✓
Mold B	✓	✓	✓
Mold C	✓	✓	✓

According to the Table 5.1 and 5.2 the materials were investigated in fired condition and 3 samples per mold were subjected to analysis for each experimental study.

5.1. Discussion of Specific Heat Results

The specific heat measurement results of the samples taken from Mold A, B and C are given in Figure 5.1.

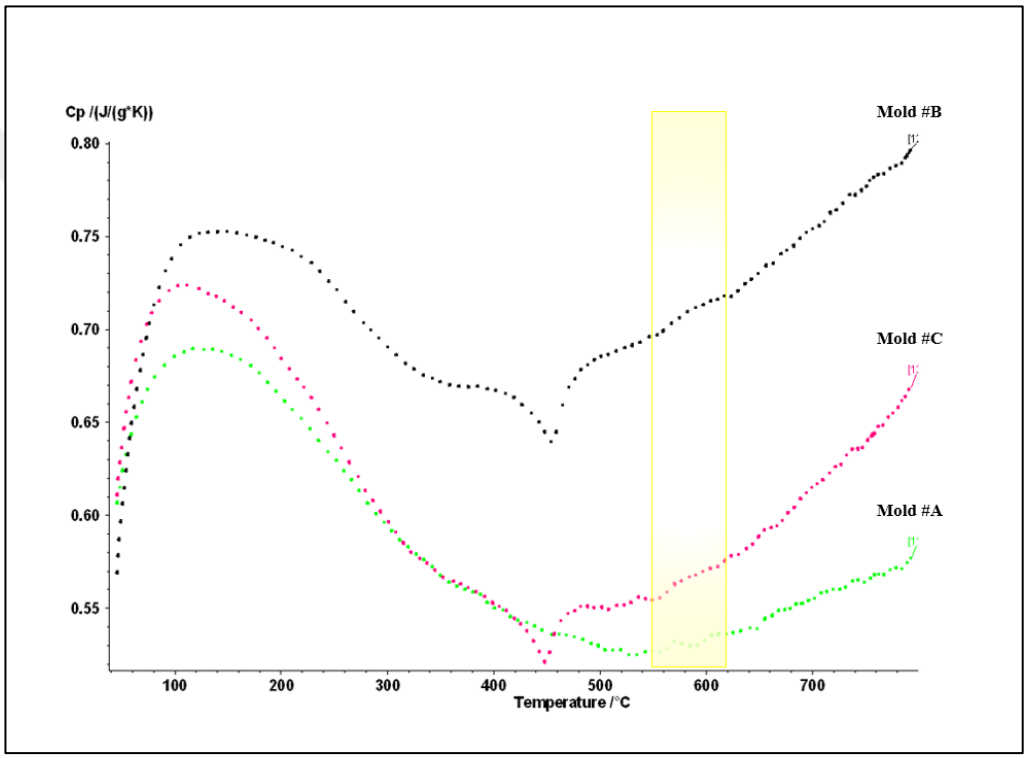

Figure 5. 1 Avg. specific heat values of Mold A, B and C samples.

As seen from Figure 5.1, it is observed that the samples show the similar behaviour with the increase in temperature. It is thought that the differences after a more sensitive approach are due to the fact that the samples are prepared with different slurry compositions. The results show that mold B samples have the highest specific heat value among the other samples. It is useful to remind that the mold B was constructed only with back-up coats without primary layer. The second highest specific heat value belongs to mold C that presentes the general application procedure of aluminum production line in Gur Metal. It is also observed that there is not a major

difference for specific heat results between Mold C and Mold A. As known, Mold A was constructed only with primary coat without back-up coats.

Since such an industrial experimental design has not been found in other studies in the literature, the specific heat values of different layer slurries cannot be compared with other researches. However, this study showed that the specific heat values of samples obtained with general application procedure remained between the specific heat results of only primary layered samples and only back-up layered samples, and since this is an expected result, it proves the reliability of the analysis.

As explained in section 4.1 the average Cp value between 572°C and 610°C is 0.5322 $\frac{J}{g\,K}$ for mold A, 0.7119 $\frac{J}{g\,K}$ for mold B and 0.7105 $\frac{J}{g\,K}$ for mold C. Based on the results given in Table 4.1, 4.2 and 4.3, it is obversed that the values vary between 0.5302 $\frac{J}{g\,K}$ and 0.7167 $\frac{J}{g\,K}$.

Since the sample to be taken as a base is mold C, its result, numerically the value of 0.7105 $\frac{J}{g\,K}$, is the specific heat value of the ceramic system produced in accordance with general application procedure for the aluminum production line.

So far, the ready data in Nova Flow&Solid simulation software database had been using to identify the mold properties. Before an investment casting part simulation was run, a value that was not validated and that did not represent the ceramic shell molding process specific to Gur Metal Investment Casting Company was entered as an input into the simulation. Figure 5.2 shows the defined data in relation to the temperature, called mold-zircon sand in Nova Flow&Solid.

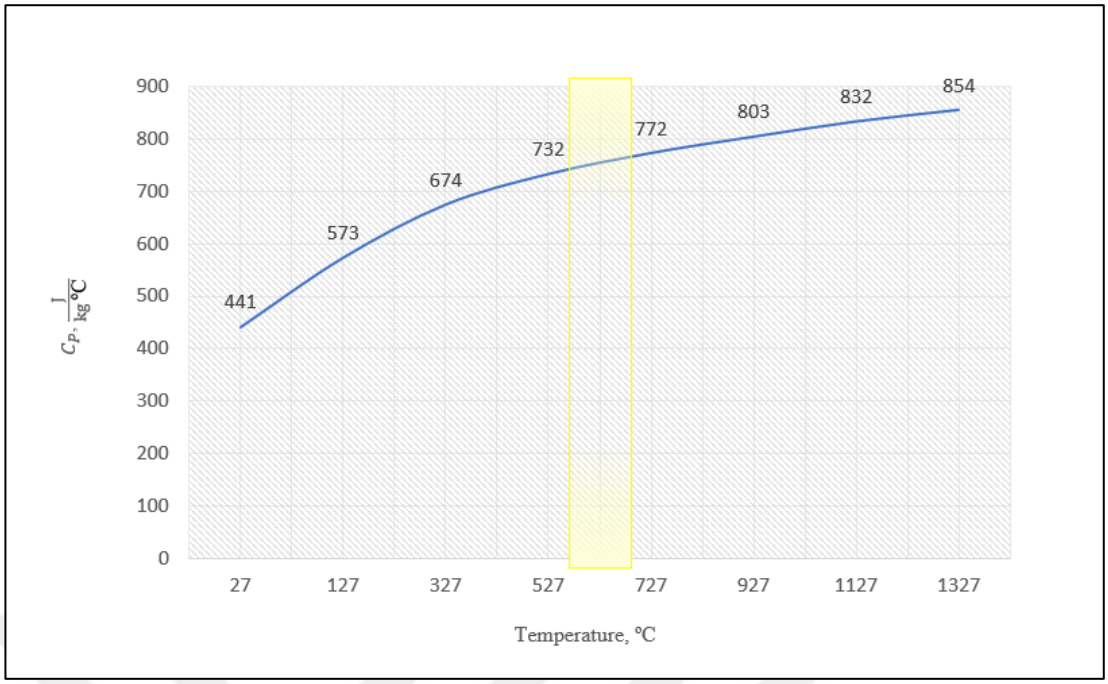

Figure 5. 2 Nova Flow&Solid database mold-zircon specific heat values.

Using the value from the database of Nova Flow&Solid is not reliable as it is not validated by the companies. The importance of making simulations with the right data was mentioned in introduction section, especially in the product development processes of difficult parts in the field of aviation, in order to use the development process efficiently and to prevent unnecessary casting trials and waste of material and energy.

Mahimkar 2011 [33] has prepared three experimental shell molds at Missouri S&T foundry and two industrial foundry shells. The author [33] prepared A) fused silica based, B) zircon and fused silica based, C) fused silica and aluminosilicate based investment casting shells. In addition to them, foundry shell A had zircon based prime coat and aluminosilicate as stucco in back-up coats and foundry shell B had fused silica based prime coat and coarser mesh silica as stucco in the back-up coats. All the shell molds were fired to 900 ºC prior to testing. The samples were analysed with laser flash test. Although different slurry compositions and stucco particles were used both in this study and the author's [33] study, the results were considered to be comparable considering the characteristics of the ceramic mold refractory materials. Specific heat values of the silica shell, silica + zircon shell and silica + aluminosilicate shell prepared at Missouri S&T foundry are higher than the specific heat of Mold A, B and C. In

addition, specific heat values of Foundry A and B industrial shell molds are even higher than silica shell, silica + zircon shell and silica + aluminosilicate shell molds. It should also noted that measurement methods were different. The author [33] used laser flash test to analysis the samples. In this study, DSC was used to analysis the samples. However, both this study and the other research [33] are on the same page about the exponential increase in Cp values depending on the temperature increase.

In another study, Konrad et al. 2011 [19] tested the specific heat values of molds with 4, 6 and 8 layers preheated at different temperatures. Different layer quantity causes the variance on the shell thicknesses. As a material, the author [19] used colloidal silica bound $ZrSiO_4$ with additions of CoAl_2O_4 for grain refinement for primary coat and mullite particles of different sizes bound by colloidal silica for back-up coats. Specific heat property of the mold was measured with two different model DSC. Mean specific heat values per devices are 1.15 $\frac{J}{g\,K}$ and 1.12 $\frac{J}{g\,K}$. They are slightly different from each other. These values are higher than the observed value in this study. However, preparation of samples and the sample compositions are different and hence this variance between the two different study values is expected.

5.2. Discussion of Density Results

The true density measurement results belongs to Mold A, B and C samples are given in Figure 5.3.

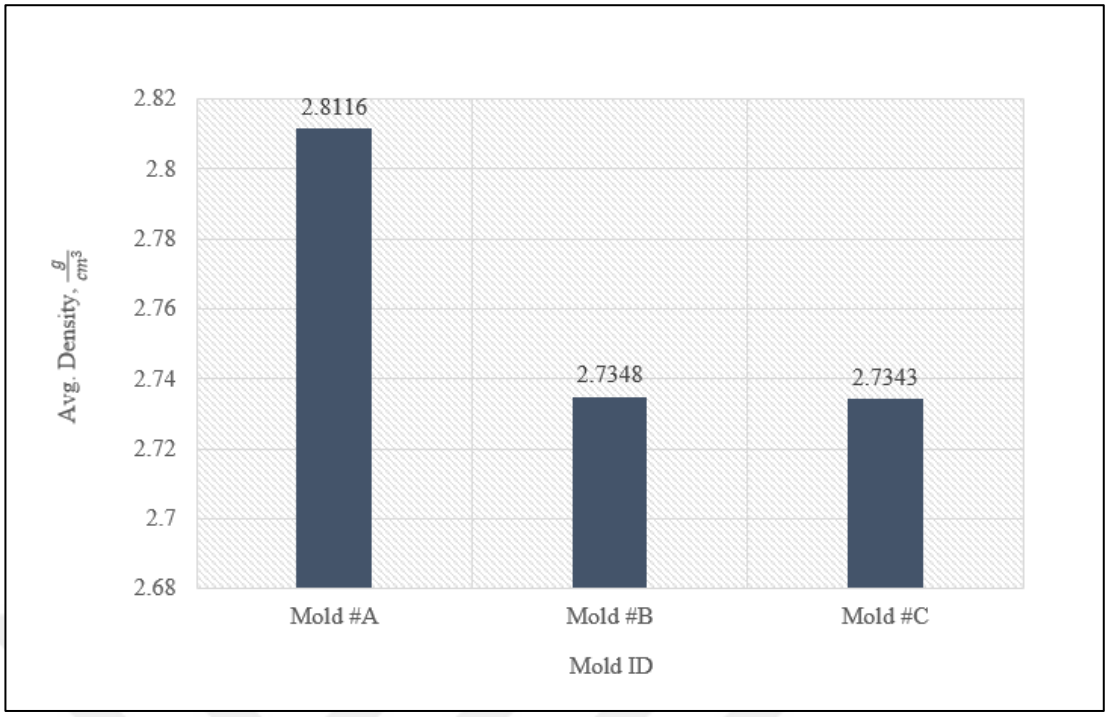

Figure 5. 3 Avg. true density values of Mold A, B and C.

As seen from the Figure 5.3, the dependence on temperature was not taken into account, as the density of the ceramic mold should only change slightly over the increasing temperature [19]. The results show that Mold A samples have the hightest density comparing to mold B and C. As known that, mold A contents only primary layer slurry. On the other hand, Mold B and C have very similar density values.

Since it is difficult to use ceramic slurries with the same contents as the samples in this study and to apply the same processing methods, it did not seem possible to come across a comparable result in the literature.

In section 4.3, the average density value is 2.8116 $\frac{g}{cm^3}$ for Mold A, 2.7348 $\frac{g}{cm^3}$ for Mold B and 2.7343 $\frac{g}{cm^3}$ for Mold C. According to the obtained results in Table 4.5, 4,7 and 4.9 density values vary between 2.3893 $\frac{g}{cm^3}$ and 3.1580 $\frac{g}{cm^3}$. In addition to true densities calculated with gas pycnometer, bulk density values were also investigated with mathematical formulas. Figure 5.4 shows the bulk density values of Mold A, B and C.

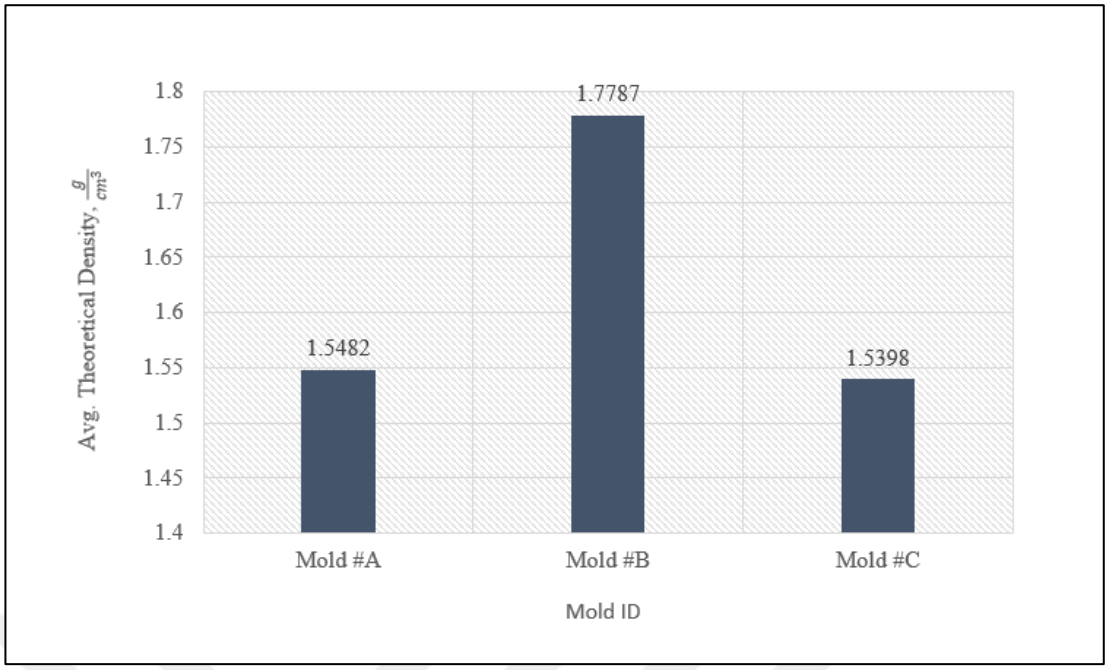

Figure 5. 4 Average bulk density values of Mold A, B and C.

The Figure 5.3 and 5.4 shows that there is a major difference between the bulk densities and true densities of each molds. The reason for this is thought to be due to the fact that the samples are in a highly porous structure, and the bulk and true values of volume are almost twice of each other.

Since the sample to be taken as a base is mold C, its result, the numerical value of 2.7343 $\frac{g}{cm^3}$ is the general application procedure ceramic system density value for the aluminum production line.

So far, the defined data in Nova Flow&Solid simulation software database had been using to identify the mold properties. Before an investment casting part simulation was run, a value that was not validated and that did not represent the ceramic shell molding process specific to Gur Metal Investment Casting Company was entered as an input into the simulation as was done for the specific heat value. Figure 5.5 shows the defined data in relation to temperature, called mold-zircon sand in Nova Flow&Solid.

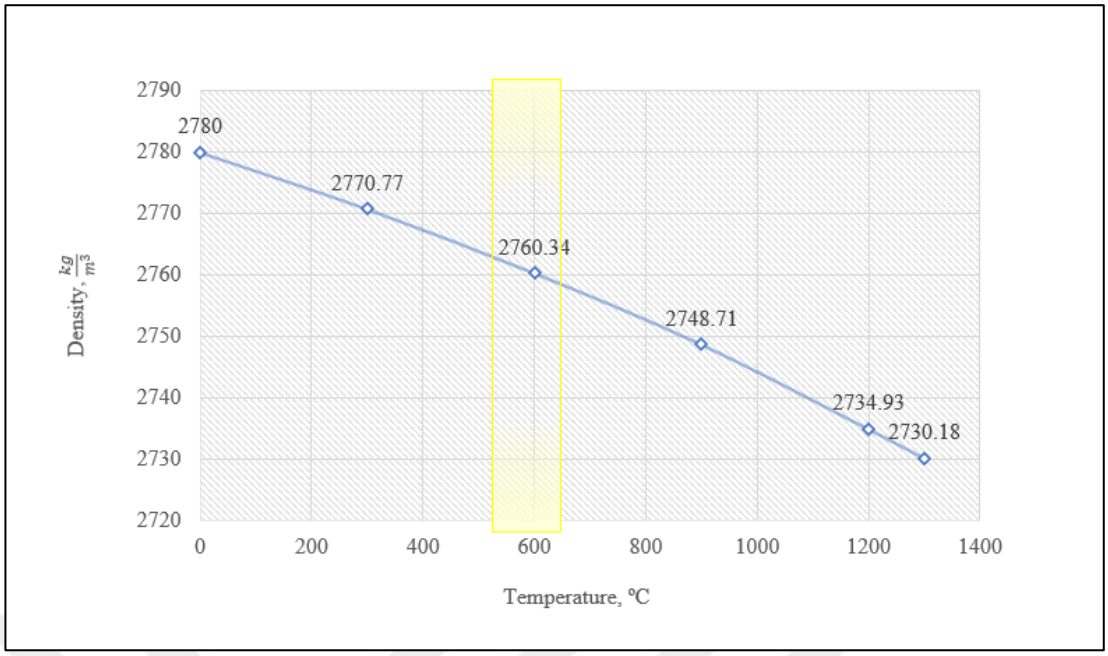

Figure 5. 5 Nova Flow&Solid database mold-zircon density values.

The use of the value in the Nova Flow&Solid database is not reliable as it is not verified by the companies. Especially in the product development processes of difficult parts in the field of aerospace, the importance of making simulations with accurate data in order to use the development processes efficiently and to avoid unnecessary casting trials and waste of matrials and energy was discussed in detail in the introduction part of this study.

5.3. Discussion of Gas Permeability Results

The avg. gas permeability measurement results of Mold A, B and C samples according to Equation 3.1 are given in Figure 5.6.

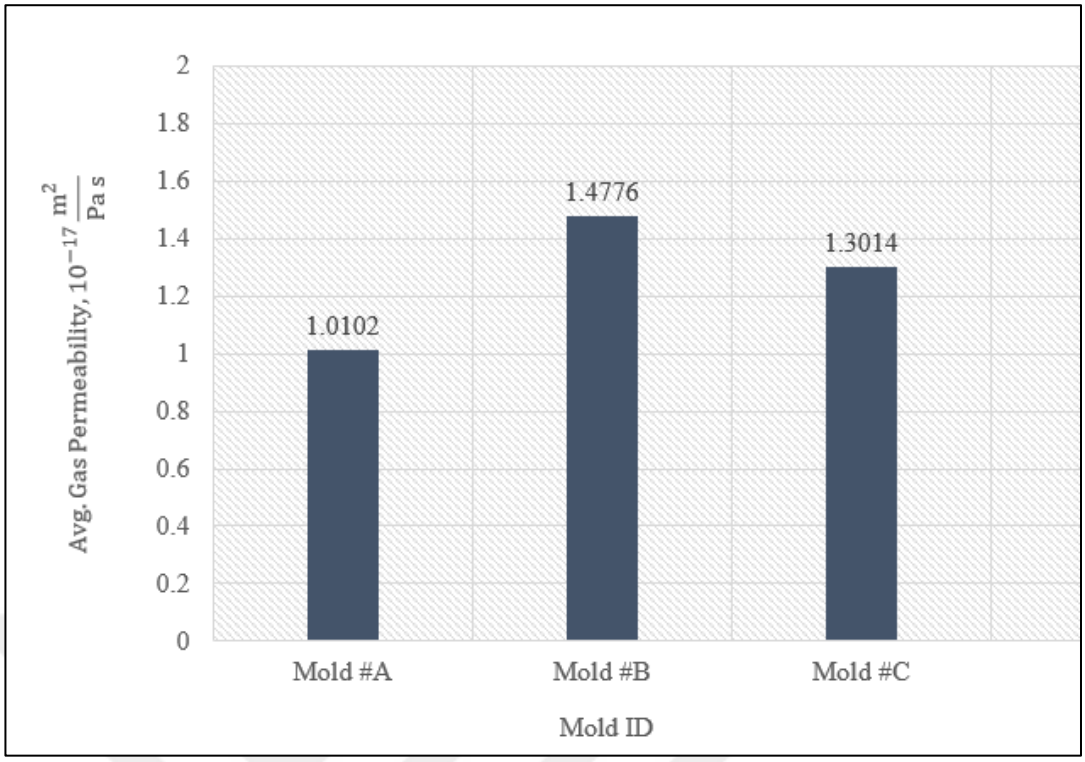

Figure 5. 6 Avg. gas permeability values of Mold A, B and C according to Equation 3.1.

The avg. gas permeability measurement results of Mold A, B and C samples according to Equation 3.2 are given in Figure 5.7.

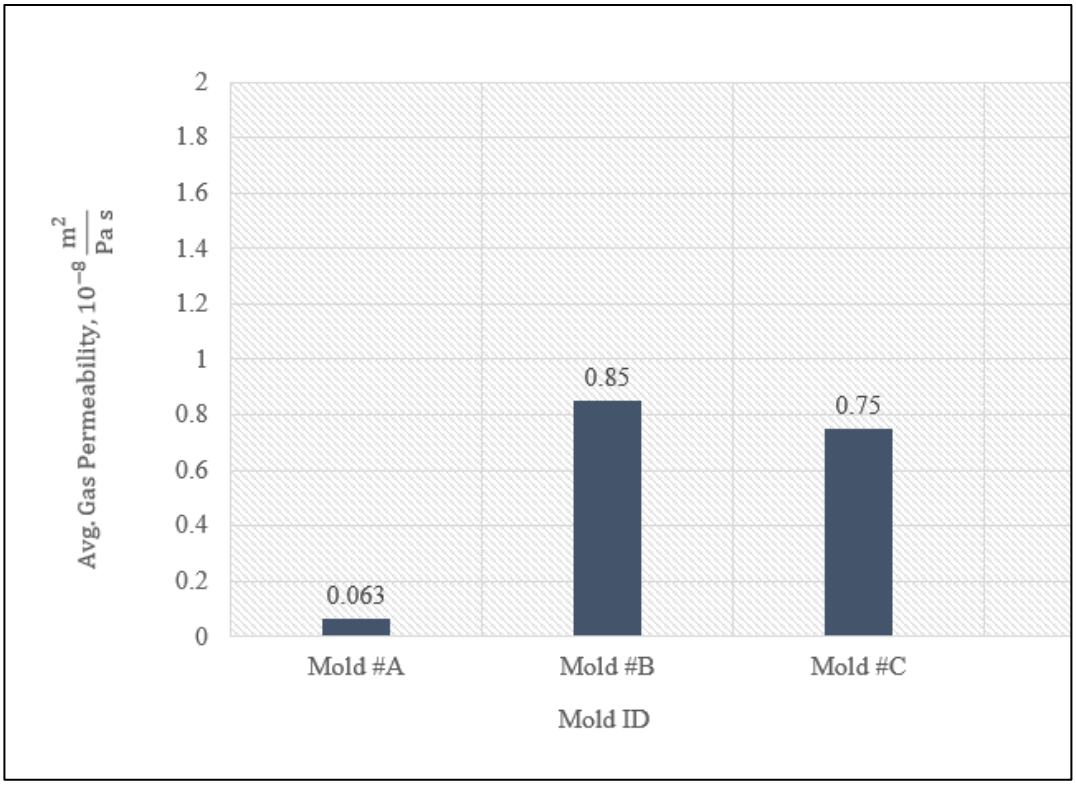

Figure 5. 7 Avg. gas permeability values of Mold A, B and C according to Equation 3.2.

As shown in Figure 5.6 and 5.7, the highest gas permeability value belongs to mold B samples which were constructed with only back-up coats. On the other hand, mold C samples have very close gas permeability value to mold B samples. The difference causes from the primary layer of mold C samples which were prepared according to aluminum production line general application procedure. Another piece of information in the figures is the value of mold A samples. Their value is lower than mold B and mold C since it has only primary coat.

The average gas permeability values for each mold type is given in section 4.4. Since the input unit of the Nova Flow & Solid casting solidification software matches the unit of the result obtained from Equation 3.2, it is also explained in section 4.4 that the calculation made with Equation 3.2 will be based. For mold A avg. gas permeability value is 0.063 x $10^{-8}\ \frac{m^2}{Pa\ s}$, for mold B it is 0.85 x $10^{-8}\ \frac{m^2}{Pa\ s}$ and for mold C it is 0.75 x $10^{-8}\ \frac{m^2}{Pa\ s}$. In general, the gas permeability interval of the molds are 0.063 - 0.85 x $10^{-8}\ \frac{m^2}{Pa\ s}$.

Mold C is the base mold that needs to be considered for the parameters. The numerical gas permeability value of this mold is 0.75 x $10^{-8}\ \frac{m^2}{Pa\ s}$ and this is the input that should feed the simulation.

However, so far, the ready data in Nova Flow&Solid simulation software database had been using to identify the mold properties as was done for specific heat and density. Before an investment casting part simulation was run, a value that was not verified and that did not represent the ceramic shell molding process specific to Gur Metal Investment Casting Company was entered as an input into the simulation. The defined data, called mold-zircon sand in Nova Flow&Solid is 2.04 x $10^{-6}\ \frac{m^2}{Pa\ s}$.

6. CONCLUSIONS AND FUTURE SCOPE

For the purpose of investigation of thermophysical properties of ceramic molds in investment casting, three molds were prepared in different ceramic shell molding composition for this study. These are Mold A) only constructed with primary layer slurry Mold B) only constructed with back-up layer slurry and Mold C) constructed with both primary and back-up layer slurry according to general application procedure of Gur Metal Investment Casting Company. Both dewaxing and burn-out processes were conducted successfully. To investigate the thermophysical properties of the molds, specific heat, density and gas permeability tests were carried out using DSC, gas-pycnometer and in-house built set-up at the laboratories. In the light of the analyzes carried out, the following results were obtained.

1) After the burn-out process, in which the wet weight is removed, the specific heat value of mold A samples, which were analyzed by DSC was determined as 0.5322 $\frac{J}{g\,K}$ between 572°C and 610°C.
2) In the same way, the specific heat value of mold B samples, which were analyzed by DSC after wet weight removal with burn-out process, was determined as 0.7119 $\frac{J}{g\,K}$ between 572°C and 610°C.
3) The same method was applied for mold C samples and the specific heat value was determined as 0.7105 $\frac{J}{g\,K}$ between 572°C and 610°C.
4) It was determined that the specific heat value of the C samples prepared according to the general application procedure of aluminum casting line in Gur Metal Investment Casting Company was between the specific heat values of the other two mold samples, A and B.
5) The result with a numerical value of 0.7105 $\frac{J}{g\,K}$ is the specific heat value of the ceramic system produced according to the general application procedure for the aluminum production line, and this value has been determined to be used in Nova Flow & Solid simulation program.

6) Density of the mold A samples that were fired was determined by gas pycnometer and it was observed that the avg. density is 2.8116 $\frac{g}{cm^3}$ at room temperature.
7) Similarly, the density of mold B samples, which were analyzed in fired condition, was determined as 2.7348 $\frac{g}{cm^3}$ at room temperature.
8) In the same way, for mold C samples the avg. density is determined as 2.7343 $\frac{g}{cm^3}$ at room temparture.
9) As a result, even though the density measurement result of the mold B samples was very close to the mold C samples, the highest density value was observed in the mold C samples.
10) It has been revealed that the experimentally generated value of 2.7343 $\frac{g}{cm^3}$ can be used in simulation runs, leaving aside the value of previously entered nonverified data in Nova Flow&Solid simulation program.
11) As a result of gas permeability analysis for mold A samples in fired condition, 0.063 x 10^{-8} $\frac{m^2}{Pa\ s}$ numerical value was determined.
12) With the same analysis method, gas permeability value was determined as 0.85 x 10^{-8} $\frac{m^2}{Pa\ s}$ for mold B samples.
13) Similarly, the gas permeability value of mold C sample was determined as 0.75 x 10^{-8} $\frac{m^2}{Pa\ s}$.
14) In the light of these gas permeability results, the highest gas permeable mold was determined as mold B and the lowest gas permeable mold was determined as mold A.
15) Since the base is mold C, 0.75 x 10^{-8} $\frac{m^2}{Pa\ s}$ value is determined for the gas permeability input for simulation runs.
16) The experimental values investigated in the scope of this study were designed to represent the standard application procedure shell molding parameters for aluminum casting line at Gur Metal Investment Casting Company.
17) Thermal conductivity measurement could not be made due to technical malfunctions in the thermal conductivity measuring device. For this reason, it is recommended to investigate the thermal conductivity of the molds and

especially to present the thermal conductivity value of mold C samples for use in simulation runs.

REFERENCES

[1] Peter Beeley, *Foundry Technology*, Second. 1972.

[2] P. R. BEELEY and SMART R.F., *Investment Casting*, Second., vol. 1. London: The Institute of Materials, 1995.

[3] Hojefa B. Dhilawala, "Investment Casting Process: Advance and Precise Casting Technique for Complex Product Design," *REST Journal on Emerging trends in Modelling and Manufacturing*, vol. 3, no. 2, pp. 29–32, 2017, [Online]. Available: www.restpublisher.com/journals/jemm

[4] S. Pattnaik, D. B. Karunakar, and P. K. Jha, "Developments in investment casting process - A review," *Journal of Materials Processing Technology*, vol. 212, no. 11. pp. 2332–2348, Nov. 2012. doi: 10.1016/j.jmatprotec.2012.06.003.

[5] S. Singh and R. Singh, "Precision investment casting: A state of art review and future trends," *Proceedings of the Institution of Mechanical Engineers, Part B: Journal of Engineering Manufacture*, vol. 230, no. 12. SAGE Publications Ltd, pp. 2143–2164, Dec. 01, 2016. doi: 10.1177/0954405415597844.

[6] S. Choudhuri and J. Shi, "Study of the Industrial Precision Manufacturing and Metallic Alloys with Respect to Economic Considerations," *Munich Personal RePEc Archive*, 2017, Accessed: May 25, 2022. [Online]. Available: https://mpra.ub.uni-muenchen.de/77481/

[7] R. Prasad, "Progress in Investment Castings," in *Science and Technology of Casting Processes*, InTech, 2012. doi: 10.5772/50550.

[8] D. MILLS, *Investment Casting*, Second., vol. 4. London: The Institute of Materials, 1995.

[9] P. Beeley, *Foundry Technology*, Second., vol. 9. Oxford: Butterworth-Heinemann, 1972.

[10] S. Jones and C. Yuan, "Advances in shell moulding for investment casting," *Materials Processing Technology*, vol. 135, pp. 258–265, 2003.

[11] Y. Venkat, K. R. Choudary, D. K. Das, A. K. Pandey, and S. Singh, "Ceramic shell moulds for investment casting of low-pressure turbine rotor blisk," *Ceramics International*, vol. 47, no. 4, pp. 5663–5670, Feb. 2021, doi: 10.1016/j.ceramint.2020.10.152.

[12] J. Bundy and S. Viswanathan, "CHARACTERIZATION OF ZIRCON-BASED SLURRIES FOR INVESTMENT CASTING," *International Journal of Metalcasting*, 2008.

[13] H. A. Mehrabi, M. R. Jolly, K. Salonitis, H. Mehrabi, M. Jolly, and K. Salonitis, "Sustainable Investment Casting Advanced structural reliability assessment for offshore wind turbine support structures based on non-intrusive stochastic methods View project Series of Handbooks in Advanced Manufacturing [ELSEVIER] View

project Sustainable Investment Casting," 2016. [Online]. Available: https://www.researchgate.net/publication/303373060

[14] W. N. dos Santos, "Experimental investigation of the effect of moisture on thermal conductivity and specific heat of porous ceramic materials," 2000.

[15] M. Xu, V. Richards, S. Lekakh, J. Smith, M. O', and K. K. Chandrashekhara, "CHARACTERIZATION OF INVESTMENT SHELL THERMAL PROPERTIES," MISSOURI UNIVERSITY OF SCIENCE AND TECHNOLOGY, Missouri, 2015.

[16] Y. C. Liu and L. S. Chao, "Modified effective specific heat method of solidification problems," *Materials Transactions*, vol. 47, no. 11, pp. 2737–2744, Nov. 2006, doi: 10.2320/matertrans.47.2737.

[17] M. Xu, S. N. Lekakh, and L. von Richards, "Thermal property database for investment casting shells," *International Journal of Metalcasting*, vol. 10, no. 3, pp. 342–347, Jul. 2016, doi: 10.1007/s40962-016-0052-4.

[18] W. N. dos Santos, "Experimental investigation of the effect of moisture on thermal conductivity and specific heat of porous ceramic materials," *Materials Science*, no. 35, pp. 3977–3982, 2000.

[19] C. H. Konrad, M. Brunner, K. Kyrgyzbaev, R. Völkl, and U. Glatzel, "Determination of heat transfer coefficient and ceramic mold material parameters for alloy IN738LC investment castings," *Journal of Materials Processing Technology*, vol. 211, no. 2, pp. 181–186, Feb. 2011, doi: 10.1016/j.jmatprotec.2010.08.031.

[20] H. Saridikmen and N. Kuskonmaz, "Properties of ceramic casting molds produced with two different binders," *Ceramics International*, vol. 31, no. 6, pp. 873–878, 2005, doi: 10.1016/j.ceramint.2004.10.004.

[21] M. Xu, S. N. Lekakh, and L. von Richards, "Thermal property database for investment casting shells," *International Journal of Metalcasting*, vol. 10, no. 3, pp. 342–347, Jul. 2016, doi: 10.1007/s40962-016-0052-4.

[22] D. M. Kline, S. N. Lekakh, and V. L. Richards, "Improving Investment Casting Mold Permeability Using Graphite Particles," in *AFS Proceedings 2010*, 2010, pp. 1–7.

[23] P. Wisniewski, R. Sitek, A. Towarek, E. Choinska, D. Moszczynska, and J. Mizera, "Molding binder influence on the porosity and gas permeability of ceramic casting molds," *Materials MDPI*, vol. 13, no. 12, Jun. 2020, doi: 10.3390/ma13122735.

[24] M. A. A. Khan and A. K. Sheikh, "Simulation tools in enhancing metal casting productivity and quality: A review," *Proceedings of the Institution of Mechanical Engineers, Part B: Journal of Engineering Manufacture*, vol. 230, no. 10, pp. 1799–1817, Oct. 2016, doi: 10.1177/0954405416640183.

[25] M. Raza, "Process development for investment casting of thin-walled components : Manufacturing of light weight components," Malardalen University , 2015.

[26] P. Tao, H. Shao, Z. Ji, H. Nan, and Q. Xu, "Numerical simulation for the investment casting process of a large-size titanium alloy thin-wall casing," *Progress in Natural Science: Materials International*, vol. 28, no. 4, pp. 520–528, Aug. 2018, doi: 10.1016/j.pnsc.2018.06.005.

[27] M. A. A. Khan and A. K. Sheikh, "A comparative study of simulation software for modelling metal casting processes," *International Journal of Simulation Modelling*, vol. 17, no. 2, pp. 197–209, Jun. 2018, doi: 10.2507/IJSIMM17(2)402.

[28] Jolly Mark, "Casting Simulation How Well Do Reality and Virtual Casting Match A State of the Art Review," *International Journal of Cast Metals Research*, vol. 14, pp. 303–313, 2002.

[29] M. A. A. Khan and A. K. Sheikh, "Simulation tools in enhancing metal casting productivity and quality: A review," *Proceedings of the Institution of Mechanical Engineers, Part B: Journal of Engineering Manufacture*, vol. 230, no. 10. SAGE Publications Ltd, pp. 1799–1817, Oct. 01, 2016. doi: 10.1177/0954405416640183.

[30] Quantachrome Instruments Anton Paar, "ULTRAPYC TRUE VOLUME AND DENSITY ANALYZER Operating Manual." [Online]. Available: www.quantachrome.com

[31] "Standard Test Method for Permeability of Refractories 1", doi: 10.1520/C0577-19.

[32] J. Zych, J. Kolczyk, and T. Snopkiewicz, "New Investigation Method of the Permeability of Ceramic Moulds Applied in the Investment Casting Technology," *Foundry Engineering*, vol. 13, no. 2, pp. 107–112, 2013.

[33] C. Mahimkar, "Thermo-physical properties measurement and steel-ceramic shell interactions in investment casting," Missouri University of Science and Technology, 2011. [Online]. Available: https://scholarsmine.mst.edu/masters_theseshttps://scholarsmine.mst.edu/masters_theses/5015

CURRICULUM VITAE

Ayça Şeyma Birdal was born in 1996 in Istanbul. She completed the Department of Metallurgical and Materials Engineering at Marmara University in 2019. She started her master's degree at Gebze Technical University, Institute of Energy Technologies, in the Department of Applied Propulsion System Design & Engineering in Aerospace Technologies in 2020 and continues. She worked as a Product Engineer in the Engineering Department at Gür Metal Investment Casting Company between 2019-2022.

Publishing Material from the Thesis:

- Birdal A.B., Aksit M, “Thermophysical Properties of Ceramic Molds”, 1st International Aerospace Propulsion System Congress 2022, Gebze, Kocaeli, Turkey, 2022

APPENDIX

APPENDIX A

Raw data of specific heat measurement DSC outputs of mold A samples between 570-610 ºC is given in Table A.1.

Table A. 1 DSC outputs of mold A samples.

Temp, °C	**Time, min.**	**Cp, $\frac{J}{g\,K}$**
570.0594	64.2	0.53212
570.3095	64.225	0.53177
570.5593	64.25	0.53123
570.8095	64.275	0.53135
571.0598	64.3	0.53122
571.3103	64.325	0.5312
571.5608	64.35	0.53174
571.8114	64.375	0.53148
572.0619	64.4	0.53137
572.3127	64.425	0.53071
572.5634	64.45	0.53053
572.8143	64.475	0.53098
573.0651	64.5	0.53124
573.3157	64.525	0.531
573.5662	64.55	0.53073
573.8167	64.575	0.53116
574.0668	64.6	0.53094
574.3169	64.625	0.53036
574.5666	64.65	0.53121
574.8164	64.675	0.53096
575.0661	64.7	0.53069
575.3156	64.725	0.53112
575.5651	64.75	0.53137
575.8146	64.775	0.53153
576.0642	64.8	0.53167
576.3139	64.825	0.53117
576.5638	64.85	0.53123
576.8139	64.875	0.53092
577.0638	64.9	0.53134
577.3138	64.925	0.53122
577.5642	64.95	0.53099
577.8145	64.975	0.53115
578.0648	65	0.53107
578.3148	65.025	0.53068

578.5647	65.05	0.53023
578.8143	65.075	0.53027
579.064	65.1	0.53043
579.3137	65.125	0.52999
579.5634	65.15	0.53071
579.8127	65.175	0.53059
580.0623	65.2	0.53062
580.3118	65.225	0.53141
580.5616	65.25	0.53105
580.8117	65.275	0.5313
581.0618	65.3	0.5312
581.3118	65.325	0.53103
581.5618	65.35	0.53127
581.812	65.375	0.53087
582.0623	65.4	0.53116
582.3124	65.425	0.53057
582.5627	65.45	0.53065
582.8127	65.475	0.53054
583.0628	65.5	0.53088
583.3129	65.525	0.53096
583.5631	65.55	0.53084
583.8133	65.575	0.53074
584.0636	65.6	0.5307
584.3137	65.625	0.53071
584.564	65.65	0.53065
584.8143	65.675	0.5306
585.0643	65.7	0.53025
585.3142	65.725	0.52959
585.5639	65.75	0.52969
585.8137	65.775	0.53
586.0635	65.8	0.53027
586.3132	65.825	0.53019
586.5627	65.85	0.53018
586.812	65.875	0.53051
587.0612	65.9	0.53068
587.3105	65.925	0.53017
587.5601	65.95	0.52976
587.8097	65.975	0.53009
588.0593	66	0.53008
588.3087	66.025	0.53048
588.5582	66.05	0.5299
588.8079	66.075	0.53027
589.0579	66.1	0.53039
589.3077	66.125	0.53
589.5577	66.15	0.53005
589.8075	66.175	0.53055
590.0574	66.2	0.53047
590.3071	66.225	0.53048

590.5566	66.25	0.53001
590.8062	66.275	0.52999
591.0556	66.3	0.53015
591.3049	66.325	0.53038
591.5543	66.35	0.53059
591.8034	66.375	0.52992
592.0525	66.4	0.53056
592.3018	66.425	0.53031
592.551	66.45	0.53069
592.8005	66.475	0.53096
593.0499	66.5	0.53078
593.2993	66.525	0.53097
593.5489	66.55	0.53048
593.7984	66.575	0.53083
594.048	66.6	0.53061
594.2976	66.625	0.53079
594.547	66.65	0.53096
594.7965	66.675	0.53117
595.0457	66.7	0.53073
595.2952	66.725	0.5311
595.5448	66.75	0.53156
595.7943	66.775	0.53127
596.0438	66.8	0.5313
596.2933	66.825	0.53134
596.5427	66.85	0.53186
596.7922	66.875	0.53186
597.0418	66.9	0.53149
597.2913	66.925	0.53204
597.5407	66.95	0.53188
597.7899	66.975	0.53236
598.0393	67	0.53225
598.2884	67.025	0.53253
598.5377	67.05	0.53261
598.7869	67.075	0.53294
599.0361	67.1	0.533
599.2854	67.125	0.53266
599.5349	67.15	0.53263
599.7842	67.175	0.53291
600.0338	67.2	0.5337
600.2833	67.225	0.5331
600.5331	67.25	0.53327
600.7829	67.275	0.5338
601.0328	67.3	0.53397
601.2826	67.325	0.53383
601.5325	67.35	0.53369
601.7826	67.375	0.53413
602.0327	67.4	0.53441
602.2826	67.425	0.53453

602.5326	67.45	0.53473
602.7824	67.475	0.53461
603.032	67.5	0.53449
603.2818	67.525	0.53478
603.5316	67.55	0.53494
603.7811	67.575	0.53527
604.0305	67.6	0.53545
604.28	67.625	0.53511
604.5295	67.65	0.53537
604.7793	67.675	0.53547
605.0291	67.7	0.5358
605.2791	67.725	0.53539
605.5289	67.75	0.53566
605.7787	67.775	0.53557
606.0287	67.8	0.53562
606.2786	67.825	0.53591
606.5284	67.85	0.53535
606.7781	67.875	0.53567
607.0277	67.9	0.53593
607.2772	67.925	0.53606
607.5267	67.95	0.53636
607.7761	67.975	0.53601
608.0256	68	0.53618
608.275	68.025	0.53682
608.5246	68.05	0.53598
608.7743	68.075	0.536
609.0241	68.1	0.53627
609.274	68.125	0.53586
609.524	68.15	0.53643
609.7741	68.175	0.53689
610.0243	68.2	0.53651
610.2744	68.225	0.53643
610.5247	68.25	0.53613
610.7748	68.275	0.53614

APPENDIX B

Raw data of specific heat measurement DSC outputs of mold B samples between 570-610 ºC is given in Table B.1.

Table B. 1 DSC outputs of mold B samples.

Temp, ºC	**Time, min.**	**Cp, $\frac{J}{g\,K}$**
570.5136	64.24387	0.70384
573.0155	64.4934	0.70515
575.5174	64.74361	0.70653
578.0193	64.99391	0.70763
580.5212	65.24455	0.70915
583.0231	65.49464	0.70991
585.525	65.74474	0.71
588.0269	65.99558	0.71141
590.5288	66.24618	0.71171
593.0307	66.49734	0.71257
595.5326	66.7483	0.71327
598.0345	66.99933	0.71372
600.5364	67.2502	0.71487
603.0383	67.50038	0.71466
605.5402	67.75068	0.7161
608.0421	68.00101	0.71674
610.544	68.25119	0.71623

APPENDIX C

Raw data of specific heat measurement DSC outputs of mold C samples between 570-610 ºC is given in Table C.1.

Table C. 1 DSC outputs of mold C samples.

Temp, ºC	**Time, min.**	**Cp, $\frac{J}{g\,K}$**
570.114	64.20368	0.56306
572.614	64.45336	0.56288
575.114	64.70318	0.56382
577.614	64.95331	0.56556
580.114	65.20347	0.56703
582.614	65.45343	0.56744
585.114	65.70331	0.56683
587.614	65.95363	0.56635
590.114	66.20384	0.56791
592.614	66.45434	0.5689
595.114	66.70477	0.56919
597.614	66.95519	0.56971
600.114	67.20576	0.57084
602.614	67.45585	0.57163
605.114	67.70615	0.57216
607.614	67.95638	0.57249
610.114	68.20657	0.57276